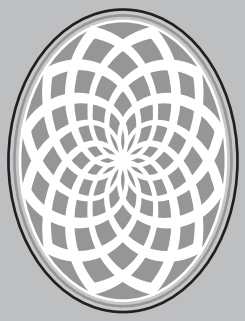

INDUSTRIAL MATHEMATICS INSTITUTE

2008:01

Analysis of a mixed finite volume discretization of fourth order equations on general surfaces

Q. Du, L. Ju and L. Tian

IMI

Preprint Series

Department of Mathematics
University of South Carolina

IMA Journal of Numerical Analysis (2005) Page 1 of 27
doi: 10.1093/imanum/dri000

Analysis of a Mixed Finite Volume Discretization of Fourth Order Equations on General Surfaces

Qiang Du*
Department of Mathematics, Pennsylvania State University,
University Park, PA 16802, USA.
Lili Ju† *and* Li Tian‡
Department of Mathematics, University of South Carolina,
Columbia, SC 29208, USA.

In this paper, we study a finite volume method for the numerical solution of a model fourth order partial differential equation defined on a smooth surface. The discretization is done via a surface mesh consisting of piecewise planar triangles and its dual surface polygonal tessellation. We provide an error estimate for the approximate solution under the H^1 norm on general regular meshes. Numerical experiments are carried out on various sample surfaces to verify the theoretical results. In addition, when the underlying mesh is constructed by the so-called constrained centroidal Voronoi meshes, we propose a numerically demonstrated superconvergent scheme to compute gradients more accurately.

Keywords: Mixed finite volume discretization, PDEs on surfaces, fourth order equations, error estimates

1. Introduction

In this paper, we consider the numerical solution of some fourth order partial differential equations defined on arbitrary surfaces or two dimensional Riemannian manifolds. PDEs of order four and higher have appeared in the mathematical models of many application problems, for example, those problems related to the surface diffusion, chemical coating, cell membrane deformation, biomedical imaging, and computer graphics [5, 6, 7, 12, 19, 26, 28, 29, 35, 40, 42]. In fact, since the computation of surface curvatures is related to the second order derivatives of the surface parameterization, the variation of curvature dependent interfacial energies (such as the bending elasticity energy) leads naturally to equilibrium conditions that are in the form of PDEs of fourth order or higher.

Motivated by the wide range of applications, various discretization techniques for fourth order PDEs on surfaces have been developed that include direct discretizations on surface meshes based on finite element methods, discrete geometric calculus, or discretizations via level set and phase field techniques for implicitly defined surfaces [2, 5, 19, 23, 26, 28, 29, 31, 34, 38, 39, 45, 46]. Meanwhile, finite volume methods have also been extensively studied for the numerical

Email: qdu@math.psu.edu. This author's research is supported in part by the National Science Foundation under grant numbers DMS-0409297 and CCF-0430349.
†*Email:* ju@math.sc.edu. This author's research is supported in part by the National Science Foundation under grant number DMS-0609575 and the Department of Energy under grant number DE-FG02-07ER64431.
‡*Email:* tianl@math.sc.edu.

solution of PDEs due to their discrete conservation properties, see for instance, [3, 4, 9, 10, 11, 13, 14, 15, 18, 24, 25, 27, 32, 33, 36, 37, 41]. Though much theoretical investigations have focused on finite volume methods for first and second order PDEs, there is relatively little discussion on the analysis of finite volume methods applied to higher order PDEs [33, 43], especially for high order PDEs defined on general surfaces. Due to the lack of comprehensive theoretical study, there have often been concerns that direct discretizations of high order PDEs based on surface triangulations may require tremendous computational effort for varying geometries and it is not clear how higher order geometric characteristics such as the derivatives of curvatures are to be well represented on triangulated surfaces [8, 28, 31]. The study presented in this paper is aimed at filling in such a gap by considering a finite volume method based on the primal-dual meshes for the numerical solution of some linear fourth order elliptic equations defined on smooth surfaces.

For an open bounded $C^{k,\alpha}$-hypersurface $\mathbf{S}$ in $\mathbb{R}^3$ [21, 30] with $k \in \mathbb{N} \cup \{0\}$ and $0 \leqslant \alpha < 1$, it may be represented globally by some oriented distance function (level set function) $d = d(\mathbf{x})$ defined in some open subset Ω of $\mathbb{R}^3$ such that $\mathbf{S} = \{\mathbf{x} \in \Omega \mid d(\mathbf{x}) = 0\}$ with $d \in C^{k,\alpha}$ and $\nabla d \neq 0$ in Ω. The unit outward normal $\vec{\mathbf{n}}(\mathbf{x}) = (n_1(\mathbf{x}), n_2(\mathbf{x}), n_3(\mathbf{x}))$ to the surface $\mathbf{S}$ (with increasing d) at $\mathbf{x}$ is given by $\vec{\mathbf{n}}(\mathbf{x}) = \nabla d(\mathbf{x})/|\nabla d(\mathbf{x})|$ where $|\cdot|$ denotes the Euclidean norm and ∇ denotes the standard gradient operator in $\mathbb{R}^3$. Without loss of generality, we assume that $|\nabla d| \equiv 1$ in Ω. Let $\nabla_s = (\nabla_{s,1}, \nabla_{s,2}, \nabla_{s,3}) = \nabla - (\vec{\mathbf{n}} \cdot \nabla)\vec{\mathbf{n}}$ denote the tangential (surface) gradient operator, and $\Delta_s = \nabla_s \cdot \nabla_s$ be the so-called Laplace-Beltrami operator on $\mathbf{S}$.

In this paper, we consider the case that $\mathbf{S}$ has no boundary, i.e., $\partial\mathbf{S} = \emptyset$, to avoid technical complication in the presentation (for $\partial\mathbf{S} \neq \emptyset$, the analysis has no essential difference with suitable boundary conditions). As an illustration of more general settings, we focus on the numerical study of the following classical fourth order elliptic problem defined on $\mathbf{S}$:

$$\Delta_s(a(\mathbf{x})\Delta_s u(\mathbf{x})) + b(\mathbf{x})u(\mathbf{x}) = f(\mathbf{x}), \quad \forall\, \mathbf{x} \in \mathbf{S}\,. \tag{1.1}$$

We assume that the surface $\mathbf{S}$ can be discretized via a surface mesh consisting of piecewise planar triangles and its dual piecewise surface polygons. Assumptions on the coefficients a and b and the right hand side f are specified later. The model equation (1.1) is much simpler than many high order PDEs associated with various applications which may be nonlinear and whose solutions may be coupled with how the surface $\mathbf{S}$ is defined or is evolving. Yet, it provides nevertheless a good starting point to illustrate the error contributions from the approximations of the surfaces and PDEs with high order surface derivatives. By adopting a second order splitting, we construct a finite volume discretization to the above equation, and provide an optimal order error estimate for the approximate solution under the H^1 norm. In addition, we also propose a scheme to compute gradients which is shown through numerical examples to display superconvergence when the underlying mesh is given by the so-called constrained centroidal Voronoi meshes. Such meshes and their practical constructions have been extensively studied in [17]. Thus, our study here serves as a justification of the feasibility and optimality of finite volume based approximations of high order PDEs defined on general surfaces. Numerical tests are also provided to validate the theoretical analysis and to offer hints on the practical performance of the finite volume schemes.

The paper is organized as follows: we first discuss the problem formulation in Section 2, then we discuss the mixed finite volume discretization in Section 3. The H^1 error analysis is presented in Section 4, and the surface mesh construction and gradient recovery are discussed in Section 5. Numerical examples and final conclusions are given in Sections 6 and 7.

2. Problem Formulation

First, we use $L^p(\mathbf{S})$, $W^{m,p}(\mathbf{S})$ and $H^m(\mathbf{S}) = W^{m,2}(\mathbf{S})$ to denote the standard Sobolev spaces on $\mathbf{S}$. It is customary to assume $k+\alpha \geqslant 1$ and $k+\alpha \geqslant m$ to make the space $H^m(\mathbf{S})$ well-defined [30]. We further assume that $\mathbf{S}$ is sufficiently smooth (say, of the class C^4) to avoid technical complications. In order to rigorously analyze the problem (1.1), the following conditions on the regularity of the coefficients are always assumed:

Assumption 1 *The coefficients of equation (1.1) satisfy that $a \in W^{2,\infty}(\mathbf{S})$, $b \in W^{1,\infty}(\mathbf{S})$, with $a(\mathbf{x}) \geqslant \alpha_1 > 0$, $b(\mathbf{x}) \geqslant \alpha_2 > 0$ for $\mathbf{x} \in \mathbf{S}$ and $f \in L^2(\mathbf{S})$.*

By introducing a new function $v = -a\Delta_s u$, the problem (1.1) then can be reduced into a problem represented by two second order equations:

$$\left\{ \begin{array}{rcl} -\Delta_s u(\mathbf{x}) - \tilde{a}(\mathbf{x})v(\mathbf{x}) & = & 0, \\ -\Delta_s v(\mathbf{x}) + b(\mathbf{x})u(\mathbf{x}) & = & f(\mathbf{x}) \end{array} \right. \tag{2.1}$$

where $\tilde{a}(\mathbf{x}) = 1/a(\mathbf{x})$ is also in $W^{2,\infty}(\mathbf{S})$. Such a reduction is naturally reminiscent to the reduction of a second order equation to first order systems which, in the finite volume setting, leads to the methods studied by [10, 14, 15, 25, 41] and the references cited therein.

For any $u, v \in H^2(\mathbf{S})$, let us define the bilinear functional $\mathcal{A}$ such that

$$\mathcal{A}(u,v) = \int_{\mathbf{S}} \nabla_s u(\mathbf{x}) \cdot \nabla_s v(\mathbf{x})\, ds.$$

We say that $(u,v) \in H^1(\mathbf{S}) \times H^1(\mathbf{S})$ is a weak solution of the equation (2.1) if and only if for any $\psi, \phi \in H^1(\mathbf{S})$,

$$\left\{ \begin{array}{rcl} \mathcal{A}(u,\psi) - (\tilde{a}v,\psi)_s & = & 0, \\ \mathcal{A}(v,\phi) + (bu,\phi)_s & = & (f,\phi)_s \end{array} \right. \tag{2.2}$$

where

$$(w,\phi)_s = \int_{\mathbf{S}} w(\mathbf{x})\phi(\mathbf{x}) ds$$

for any $w \in L^2(\mathbf{S})$.

First, we state some results on the well-posedness in the following theorem.

Theorem 1 *Under the Assumption 1, there exists a generic constant $c > 0$ such that for every $f \in L^2(\mathbf{S})$, there exists a unique solution $(u,v) \in H^2(\mathbf{S}) \times H^2(\mathbf{S})$ for the equation (2.1), and (u,v) satisfies the following estimate:*

$$\|u\|_{H^2(\mathbf{S})} + \|v\|_{H^2(\mathbf{S})} \leqslant c\|f\|_{L^2(\mathbf{S})}\,. \tag{2.3}$$

The existence of weak solution u in $H^2(\mathbf{S})$ and its H^2 bound can be proved using the standard Lax-Milgram theorem and the Sobolev embedding results for spaces defined on a compact manifold [30]. The bound on v can then be derived from regularlity estimates for second order elliptic equations, as those corresponding to (2.2), on the manifold $\mathbf{S}$ [1].

3. Mixed Finite Volume Discretization

We now present a mixed finite volume discretization of the equation (1.1). To make notation simple, we now summarize some glossaries that are used later. More precise definitions are to be found in the rest of the section.

3.1 *Meshes and discrete spaces*

Denote $\mathcal{T} = \{T_i\}_{i=1}^m$ and $\mathcal{T}^h = \{T_i^h\}_{i=1}^m$ to be the curved and planar triangulations of the surface $\mathbf{S}$ and its piecewise polygonal approximation $\mathbf{S}^h$ respectively. As defined later, these triangulations are related to each other by a lift map $\mathcal{L}$ from $\mathbf{S}^h$ to $\mathbf{S}$; $\mathcal{K}$ and $\mathcal{K}^h$ are the corresponding dual tessellations of $\mathbf{S}$ and $\mathbf{S}^h$; $\mathcal{U}$ and $\mathcal{V}$ denote piecewise linear and piecewise constant function spaces defined on the triangulation $\mathbf{S}^h$ and tessellation $\mathcal{K}^h$ respectively; $\mathit{\Pi}_u$ and $\mathit{\Pi}_v$ are interpolation operators into $\mathcal{U}$ and $\mathcal{V}$ respectively, while π_u and π_v are the counterparts onto the pair of spaces induced by $\mathcal{U}$ and $\mathcal{V}$ on $\mathbf{S}$ through the lift $\mathcal{L}$; $\mathbf{P}_h$ and $\mathbf{P}$ are some projection operators; $\mathcal{A}$, $\mathcal{A}_G^h$, and $\mathcal{A}_G$ denote some bilinear forms with the subscript G symbolizing the use of Green's formula in the definition.

For the smooth surface $\mathbf{S}$, we may assume that there is a strip (*band*)

$$\mathbf{U} = \{\mathbf{x} \in \mathit{\Omega} \mid dist(\mathbf{x}, \mathbf{S}) < \delta\}$$

around $\mathbf{S}$ for some $\delta > 0$ such that there is a unique decomposition $\mathbf{x} = \mathbf{p}(\mathbf{x}) + d(\mathbf{x})\vec{\mathbf{n}}(\mathbf{x})$ for any $\mathbf{x} \in \mathbf{U}$, where $\mathbf{p}(\mathbf{x}) \in \mathbf{S}$ and $d(\mathbf{x})$ is the signed distance to $\mathbf{S}$, and $\vec{\mathbf{n}}(\mathbf{x})$ denotes the unit outward normal of $\mathbf{S}$ at $\mathbf{p}(\mathbf{x})$. The parameter δ may be determined via the surface curvatures if $\mathbf{S}$ is sufficiently smooth. Then, a function u defined on $\mathbf{S}$ can be extended uniquely in the strip by

$$U(\mathbf{x}) = u(\mathbf{p}(\mathbf{x})) = u(\mathbf{x} - d(\mathbf{x})\vec{\mathbf{n}}(\mathbf{x})), \quad \forall\, \mathbf{x} \in \mathbf{U}.$$

Let $\mathbf{S}$ be approximated by a sequence of continuous piecewise linear complex $\{\mathbf{S}^h \subset \mathbf{U}\}$ which consists of a sequence of regular triangulations $\{\mathcal{T}^h = \{T_i^h\}_{i=1}^m\}$ with $h \searrow 0$ denoting the mesh parameter. Each $\mathcal{T}^h$ contains vertices $\{\mathbf{x}_i\}_{i=1}^n$ on $\mathbf{S}$ (i.e., $\{\mathbf{x}_i\}_{i=1}^n \subset \mathbf{S} \cap \mathbf{S}^h$), see Fig. 1 (left). Clearly, $\mathbf{S}^h$ is globally of the class $C^{0,1}$. We use $m(\cdot)$ to denote the area for planar regions or the length for arcs and segments.

We assume that $\mathcal{T}^h$ satisfies the following mesh regularity condition:

$$c_1 h^2 \leqslant m(T_i^h) \leqslant c_2 h^2 \tag{3.1}$$

where h is the mesh parameter (size) for $\mathcal{T}^h$, c_1 and c_2 are some positive constants independent of h. By the uniqueness of the vector decomposition discussed above, we define $T_i = \{\mathbf{p}(\mathbf{x}) \in \mathbf{S} \mid \mathbf{x} \in T_i^h\}$ and let $\mathcal{T} = \{T_i\}_{i=1}^m$, then $\mathbf{S} = \cup_{i=1}^m T_i$.

Let $\nabla_{s_h} = (\nabla_{s_h,1}, \nabla_{s_h,2}, \nabla_{s_h,3}) = \nabla - \vec{\mathbf{n}}_h(\vec{\mathbf{n}}_h \cdot \nabla)$ be the tangential gradient operator on $\mathbf{S}^h$ where $\vec{\mathbf{n}}_h(\mathbf{x}) = (n_{h1}(\mathbf{x}), n_{h2}(\mathbf{x}), n_{h3}(\mathbf{x}))$ is the unit outward normal to $\mathbf{S}^h$. Since $\vec{\mathbf{n}}_h$ is constant on each planar triangle T_i^h, ∇_{s_h} only needs to be locally defined as a two dimensional gradient operator on the plane formed by T_i^h, and the Sobolev space $W^{m,p}(\mathbf{S}^h)$ is well-defined for $m \leqslant 1$.

We take the strategy similar to that adopted in [21, 22] to numerically solve the equation on $\mathbf{S}^h$ instead of $\mathbf{S}$. We will directly discretize the equation (2.1) (the mixed form) instead of the original problem (1.1) using a finite volume method [11, 33] (also named a finite volume element method, see for instance, [9, 24, 44]). To compare the discrete solution on $\mathbf{S}^h$ with the continuous exact solution on $\mathbf{S}$, we lift a function U defined on $\mathbf{S}^h$ to $\mathbf{S}$ by

$$\mathcal{L} : U \to u = \mathcal{L}(U) \;\text{ where }\; u(\mathbf{y}) = U(\mathbf{p}^{-1}(\mathbf{y})), \quad \forall\, \mathbf{y} \in \mathbf{S}, \tag{3.2}$$

that is, $U(\mathbf{x}) = u(\mathbf{p}(\mathbf{x})) = u(\mathbf{x} - d(\mathbf{x})\vec{\mathbf{n}}(\mathbf{x}))$ for $\mathbf{x} \in \mathbf{S}^h$.

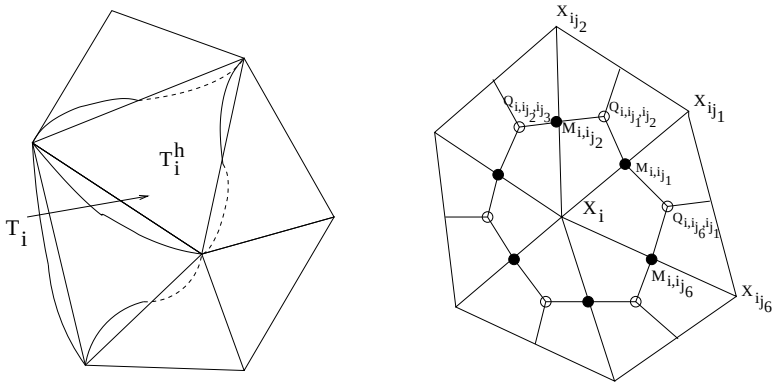

FIG. 1. Approximate mesh surface and the control volume.

Before discussing the discretization scheme, we first project the coefficients and the data $\tilde{a}$, b and f in (2.1) from $\mathbf{S}$ onto $\mathbf{S}^h$ by $\tilde{A} = \mathcal{L}^{-1}(\tilde{a})$, $B = \mathcal{L}^{-1}(b)$, and $F = \mathcal{L}^{-1}(f)$. Since $\mathbf{S}$ is sufficiently smooth, it is easy to find that $\tilde{A}, B \in W^{1,\infty}(T_i^h)$ and $F \in L^2(T_i^h)$ for any $T_i^h \in \mathcal{T}^h$ and

$$\|\tilde{A}\|_{W^{1,\infty}(T_i^h)} < c_1 \|\tilde{a}\|_{W^{1,\infty}(\mathbf{S})}, \quad \|B\|_{W^{1,\infty}(T_i^h)} < c_2 \|b\|_{W^{1,\infty}(\mathbf{S})}.$$

for some positive constants $c_1, c_2 > 0$.

Let $\mathcal{U}$ be the space of continuous piecewise linear polynomials on $\mathbf{S}^h$ with respect to $\mathcal{T}^h$,

$$\mathcal{U} = \{U^h \in C^0(\mathbf{S}^h) \ \mid \ U^h|_{T_i^h} \in \mathbb{P}_1(T_i^h)\}$$

where $\mathbb{P}_k(D)$ denotes the space of polynomials of degree no larger than k on any planar domain D. It is easy to see that $\mathcal{U} \subset H^1(\mathbf{S}^h)$ and for $U^h \in \mathcal{U}$ we have that $\nabla_{s_h} U^h$ is constant on each triangle $T_i^h \in \mathcal{T}^h$. A dual tessellation of $\mathcal{T}^h$ on $\mathbf{S}^h$ can be defined as seen in Fig. 1 (right). For each vertex $\mathbf{x}_i$, let $\chi_i = \{i_s\}_{s=1}^{m_i}$ be the set of indices of its neighbors, $Q_{i,i_j,i_{j+1}}$ (where $i_{s+1} = i_1$ if $s = m_i$) be the centroid of the triangle $\triangle \mathbf{x}_i \mathbf{x}_{i_j} \mathbf{x}_{i_{j+1}}$ and M_{i,i_j} be the midpoint of $\overline{\mathbf{x}_i \mathbf{x}_{i_j}}$ for $i_j \in \chi_i$. Let $K_i^h = \cup_{i_j \in \chi_i} \Omega_{i,i_j,i_{j+1}}$ where $\Omega_{i,i_j,i_{j+1}}$ denotes the polygonal region bounded by $\mathbf{x}_i$, M_{i,i_j}, $Q_{i,i_j,i_{j+1}}$ and $M_{i,i_{j+1}}$. In general, K_i^h is only piecewise planar and we define its projection on $\mathbf{S}$ by $K_i = \{\mathbf{p}(\mathbf{x}) \in \mathbf{S} \mid \mathbf{x} \in K_i^h\}$. Let σ denote the set of indices of all the vertices of $\mathcal{T}^h$, then, $\mathcal{K} = \{K_i\}_{i \in \sigma}$ and $\mathcal{K}^h = \{K_i^h\}_{i \in \sigma}$ may be viewed as dual tessellations of $\mathbf{S} = \cup_{i=1}^m T_i$ and $\mathbf{S}^h = \cup_{i=1}^m T_i^h$. In the remaining part of this paper, for simplicity, we will let i_j mean $i_{(j-1) \bmod(m_i)+1}$ if $j > m_i$ when $i_j \in \chi_i$ ($\mathbf{x}_{i_j}$ is a neighbor vertex of $\mathbf{x}_i$), otherwise i_j will mean $i_{(j-1) \bmod(3)+1}$ if $j > 3$ when $\mathbf{x}_{i_j}$ is a vertex of $T_i^h = \triangle \mathbf{x}_{i_1} \mathbf{x}_{i_2} \mathbf{x}_{i_3}$.

Denote by $\mathcal{V}$ the space of grid functions on $\mathbf{S}^h$ with respect to $\mathcal{K}^h$:

$$\mathcal{V} = \{\Gamma^h \ \mid \ \Gamma^h|_{K_i^h} \in \mathbb{P}_0(K_i^h)\}.$$

A set of basis functions $\{\Psi_i^h\}_{i \in \sigma}$ of $\mathcal{V}$ is given by

$$\Psi_i^h(\mathbf{x}) = \begin{cases} 1, & \mathbf{x} \in K_i^h; \\ 0, & \mathbf{x} \in \mathbf{S}^h - K_i^h. \end{cases}$$

3.2 *A discrete bilinear form and the finite volume scheme*

For any $\phi^h \in \mathcal{V}$ and $U \in H^1(\mathbf{S}^h)$ with $U|_{T_i^h} \in H^2(T_i^h)$ for any $T_i^h \in \mathcal{T}^h$, let us define the bilinear functional $\mathcal{A}_G^h$ as

$$\mathcal{A}_G^h(U, \phi^h) = \sum_{i\in\sigma} \phi_i^h \mathcal{A}_G^h(U, \Psi_i^h)$$

where $\phi_i^h = \phi^h(\mathbf{x}_i)$ and

$$\begin{aligned} \mathcal{A}_G^h(U, \Psi_i^h) &= -\int_{\partial K_i^h} \nabla_{s_h} U(\mathbf{x}) \cdot \vec{\mathbf{n}}_{K_i^h} d\gamma_h \\ &= -\sum_{i_j\in\chi_i} \int_{\Gamma_{i,i_j,i_{j+1}}} \nabla_{s_h} U(\mathbf{x}) \cdot \vec{\mathbf{n}}_{K_i^h} d\gamma_h \end{aligned}$$

with $\Gamma_{i,i_j,i_{j+1}} = \partial K_i^h \cap \triangle \mathbf{x}_i \mathbf{x}_{i_j} \mathbf{x}_{i_{j+1}} = \overline{M_{i,i_j} Q_{i,i_j,i_{j+1}} M_{i,i_{j+1}}}$ and $\vec{\mathbf{n}}_{K_i^h}$ denoting the outward unit normal of ∂K_i^h. Then the *mixed finite volume discretization* for the fourth order equation (1.1) is given by: find $(U^h, V^h) \in \mathcal{U} \times \mathcal{U}$ such that

$$\left\{ \begin{array}{rcll} \mathcal{A}_G^h(U^h, \psi^h) - (\tilde{A}V^h, \psi^h)_{s_h} &=& 0, & \\ \mathcal{A}_G^h(V^h, \phi^h) + (BU^h, \phi^h)_{s_h} &=& (F, \phi^h)_{s_h}, & \forall\ \psi^h, \phi^h \in \mathcal{V}\,, \end{array} \right. \tag{3.3}$$

where

$$(U, W)_{s_h} = \int_{\mathbf{S}^h} U(\mathbf{x}) W(\mathbf{x}) ds_h$$

for any U and W in $L^2(\mathbf{S}^h)$.

3.3 *A mass-lumping scheme*

In practical implementation, we first notice that U^h is piecewise linear on $\mathbf{S}^h$ with respect to $\mathcal{T}^h$ and $\nabla_{s_h} U^h$ is constant on each triangle $\triangle \mathbf{x}_i \mathbf{x}_{i_j} \mathbf{x}_{i_{j+1}}$. Defining

$$\tilde{A}_i = \frac{1}{m(K_i^h)} \int_{K_i^h} \tilde{A}(\mathbf{x}) ds_h, \quad B_i = \frac{1}{m(K_i^h)} \int_{K_i^h} B(\mathbf{x}) ds_h, \quad F_i = \frac{1}{m(K_i^h)} \int_{K_i^h} F(\mathbf{x}) ds_h$$

as averages over K_i^h, we then use the following approximations:

$$\begin{aligned} (\tilde{A}V^h, \psi^h)_{s_h} &= \int_{\mathbf{S}^h} \tilde{A}(\mathbf{x}) V^h(\mathbf{x}) \psi^h(\mathbf{x}) ds_h \approx \sum_{i\in\sigma} m(K_i^h) \tilde{A}_i V_i^h \psi_i^h, \\ (BU^h, \phi^h)_{s_h} &= \int_{\mathbf{S}^h} B(\mathbf{x}) U^h(\mathbf{x}) \phi^h(\mathbf{x}) ds_h \approx \sum_{i\in\sigma} m(K_i^h) B_i U_i^h \phi_i^h, \\ (F, \phi^h)_{s_h} &= \int_{S^h} F(\mathbf{x}) \phi^h(\mathbf{x}) ds_h \approx \sum_{i\in\sigma} m(K_i^h) F_i \phi_i^h \end{aligned}$$

where $V_i^h = V^h(\mathbf{x}_i)$ and $U_i^h = U^h(\mathbf{x}_i)$. Additionally,

$$\mathcal{A}_G^h(U^h, \psi^h) = \sum_{i\in\sigma} \psi_i^h \mathcal{A}_G^h(U^h, \Psi_i^h)$$

and with some careful calculations [33], we can find that

$$\begin{aligned}\mathcal{A}_G^h(U^h,\Psi_i^h) &= -\sum_{i_j\in\chi_i}[q^1_{i,i_j,i_{j+1}}(U^h_{i_j}-U^h_i)+q^2_{i,i_j,i_{j+1}}(U^h_{i_{j+1}}-U^h_i)]\\ &= -\sum_{i_j\in\chi_i} p_{i,i_j}(U^h_{i_j}-U^h_i),\end{aligned}$$

where $p_{i,i_j}=q^1_{i,i_j,i_{j+1}}+q^2_{i,i_{j-1},i_j}$ and

$$\begin{aligned}q^k_{i,i_j,i_{j+1}} &= \frac{1}{8m(\Delta\mathbf{x}_i\mathbf{x}_{i_j}\mathbf{x}_{i_{j+1}})}\left((-1)^{k-1}|\mathbf{x}_{i_{j+1}}-\mathbf{x}_i|^2\right.\\ &\qquad\left.+(-1)^k|\mathbf{x}_{i_j}-\mathbf{x}_i|^2+|\mathbf{x}_{i_j}-\mathbf{x}_{i_{j+1}}|^2\right),\quad k=1,2\end{aligned}$$

are contants depending only on the geometry of the surface triangulation $\mathcal{T}^h$.

With the numerical integration discussed above, we may transform (3.3) to the following linear system: for all $i\in\sigma$,

$$\left\{\begin{array}{rcl}-\sum_{i_j\in\chi_i}p_{i,i_j}(U^h_{i_j}-U^h_i)-m(K^h_i)\tilde{A}_iV^h_i &=& 0,\\ -\sum_{i_j\in\chi_i}p_{i,i_j}(V^h_{i_j}-V^h_i)+m(K^h_i)B_iU^h_i &=& m(K^h_i)F_i.\end{array}\right. \tag{3.4}$$

Remark 1 *In this paper, we only analyze the error of the finite volume approximation (3.3). The above mass-lumped integration rule (3.4) turns out to be very effective in practical implementations as demonstrated by our numerical experiments. The analysis given below can be generalized to (3.4), but similar to [18], more stringent regularity assumptions on the data and the exact solution would be required.*

3.4 *Some technical lemmas*

Let us define some discrete inner products and norms associated with $\mathcal{T}^h$ and a particular triangle $T^h_i=\triangle\mathbf{x}_{i_1}\mathbf{x}_{i_2}\mathbf{x}_{i_3}\in\mathcal{T}^h$ as follows:

$$\left\{\begin{array}{l}(U^h,V^h)_{T^h_i}=\dfrac{1}{3}m(T^h_i)(\sum_{j=1}^3U^h(\mathbf{x}_{i_j})V^h(\mathbf{x}_{i_j})),\ (U^h,V^h)_{\mathcal{T}^h}=\sum\limits_{T^h_i\in\mathcal{T}^h}(U^h,V^h)_{T^h_i},\\ \|U^h\|^2_{0,T^h_i}=(U^h,U^h)_{T^h_i},\quad |U^h|^2_{1,T^h_i}=m(T^h_i)\left|\nabla_{s_h}U^h|_{T^h_i}\right|^2,\ |U^h|^2_{1,\mathcal{T}^h}=\sum_{T^h_i\in\mathcal{T}^h}|U^h|^2_{1,T^h_i}\end{array}\right.$$

and $\|U^h\|^2_{0,\mathcal{T}^h}=(U^h,U^h)_{\mathcal{T}^h}$, $\|U^h\|^2_{1,\mathcal{T}^h}=\|U^h\|^2_{0,\mathcal{T}^h}+|U^h|^2_{1,\mathcal{T}^h}$.

Thanks to the fact $Q_{i_1i_2i_3}$ is chosen to be the centroid of $\triangle\mathbf{x}_{i_1}\mathbf{x}_{i_2}\mathbf{x}_{i_3}$, we also have [33]

$$\|U^h\|^2_{0,\mathcal{T}^h}=(U^h,U^h)_{\mathcal{T}^h}=\sum_{i\in\sigma}m(K^h_i)(U^h(\mathbf{x}_i))^2.$$

As the norms are defined locally on piecewise planar triangles, the following technical lemma is a trivial generalization of the same result given in [33].

Lemma 1 *There exist some generic constants $c_1,c_2>0$ such that for any $U^h\in\mathcal{U}$,*

$$\begin{aligned}c_1\|U^h\|_{0,\mathcal{T}^h}\leqslant\|U^h\|_{L^2(\mathbf{S}^h)}\leqslant c_2\|U^h\|_{0,\mathcal{T}^h},\\ c_1\|U^h\|_{1,\mathcal{T}^h}\leqslant\|U^h\|_{H^1(\mathbf{S}^h)}\leqslant c_2\|U^h\|_{1,\mathcal{T}^h}.\end{aligned}$$

For any $U \in C^0(\mathbf{S}^h)$, denote by $\Pi_u(U)$ the interpolation of U onto $\mathcal{U}$ and by $\Pi_v(U)$ the interpolation onto $\mathcal{V}$, i.e., $\Pi_u(U) \in \mathcal{U}$, $\Pi_v(U) \in \mathcal{V}$ and

$$\Pi_u(U)(\mathbf{x}_i) = U(\mathbf{x}_i) = \Pi_v(U)(\mathbf{x}_i)$$

for all $i \in \sigma$. Then, we have the following classic approximation results:

Lemma 2 *If $U \in H^2(T_i^h)$ for all $T_i^h \in \mathcal{T}^h$, then there exist some generic constants $c_1, c_2 > 0$ such that for any $T_i^h \in \mathcal{T}^h$,*

$$\|U - \Pi_u(U)\|_{L^2(T_i^h)} + h\|U - \Pi_u(U)\|_{H^1(T_i^h)} \leqslant c_1 h^2 \|U\|_{H^2(T_i^h)},$$
$$\|U - \Pi_u(U)\|_{L^2(T_i^h)} \leqslant c_2 h \|U\|_{H^1(T_i^h)}.$$

The symmetry of the bilinear form $\mathcal{A}_G^h(\cdot, \Pi_v(\cdot))$ in $\mathcal{U} \times \mathcal{U}$ can be verified as follows.

Lemma 3 *For any $U^h, V^h \in \mathcal{U}$,*

$$\mathcal{A}_G^h(U^h, \Pi_v(V^h)) = \int_{\mathbf{S}^h} \nabla_{s_h} U^h \cdot \nabla_{s_h} V^h d\mathbf{x} = \mathcal{A}_G^h(V^h, \Pi_v(U^h)) \,.$$

Proof: Let $T_i^h = \triangle \mathbf{x}_{i_1} \mathbf{x}_{i_2} \mathbf{x}_{i_3}$, we have

$$\begin{aligned} \mathcal{A}_G^h(U^h, \Pi_v(V^h)) &= \sum_{i \in \sigma} V_i^h \mathcal{A}_G^h(U^h, \Psi_i^h) = -\sum_{i \in \sigma} \sum_{i_j \in \chi_i} V_i^h \int_{\Gamma_{i,i_j,i_{j+1}}} \nabla_{s_h} U^h(\mathbf{x}) \cdot \vec{\mathbf{n}}_{K_i^h} d\gamma_h \\ &= \sum_{T_i^h \in \mathcal{T}^h} \left(-\sum_{j=1}^{3} V_{i_j}^h \int_{\partial K_{i_j}^h \cap T_i^h} \nabla_{s_h} U^h(\mathbf{x}) \cdot \vec{\mathbf{n}}_{K_{i_j}^h} d\gamma_h \right). \end{aligned}$$

Note that each T_i^h can be regarded as a triangle in xy-plane with some suitable affine mapping and ∇_{s_h} as the standard two-dimensional gradient operator, then noticing that the result from [33] (Theorem 3.2.1 on page 125) remains valid even though there are jumps in the normals between adjacent triangles, we may apply it to get

$$\mathcal{A}_G^h(U^h, \Pi_v(V^h)) = \sum_{T_i^h \in \mathcal{T}^h} m(T_i^h)(\nabla_{s_h} U^h \mid_{T_i^h} \cdot \nabla_{s_h} V^h \mid_{T_i^h}) = \int_{\mathbf{S}^h} \nabla_{s_h} U^h \cdot \nabla_{s_h} V^h ds_h$$

which gives us the desired conclusion. □

Note that the result of the above lemma is in fact a statement on the interesting connection between the finite volume and the standard linear finite element discretizations of the surface Laplace-Betrami operator. From the proof of the lemma, we also see that

Proposition 1 *For any $U^h \in \mathcal{U}$,*

$$\mathcal{A}_G^h(U^h, \Pi_v(U^h)) = |U^h|^2_{H^1(\mathbf{S}^h)} \,.$$

The following lemma shows the equivalence of $\|\cdot\|^2_{L^2(\mathbf{S}^h)}$ and $(\cdot, \Pi_v(\cdot))_{s_h}$ on $\mathcal{U}$.

Lemma 4 *Let $r(\mathbf{x})$ be a function defined on $\mathbf{S}$ with $r \in W^{1,\infty}(\mathbf{S})$ and $r(\mathbf{x}) > \alpha$ for some constant $\alpha > 0$. Let $R = \mathcal{L}^{-1}(r)$. Then there exist some generic constants $c_1, c_2 > 0$ such that*

$$c_1\|U^h\|^2_{L^2(\mathbf{S}^h)} \leqslant (RU^h, \Pi_v(U^h))_{s_h} \leqslant c_2\|U^h\|^2_{L^2(\mathbf{S}^h)}$$

for any $U^h \in \mathcal{U}$ when h is sufficiently small.

Proof: It has been shown in [33] (Lemma 4.1.1, p.191) that for any $\mathcal{T}_i^h = \triangle \mathbf{x}_{i_1}\mathbf{x}_{i_2}\mathbf{x}_{i_3} \in \mathcal{T}^h$,

$$(U^h, \Pi_v(U^h))_{T_i^h} \quad = \quad m(T_i^h)[U_{i_1}^h, U_{i_2}^h, U_{i_3}^h]\mathbf{M}[U_{i_1}^h, U_{i_2}^h, U_{i_3}^h]^T$$

with a positive definite matrix

$$\mathbf{M} = \frac{1}{108}\begin{bmatrix} 22 & 7 & 7 \\ 7 & 22 & 7 \\ 7 & 7 & 22 \end{bmatrix}.$$

Thus there exist some generic constants $c_1, c_2 > 0$, independent of h, such that

$$c_3\|U^h\|^2_{0,\mathcal{T}_i^h} \leqslant (U^h, \Pi_v(U^h))_{T_i^h} \leqslant c_4\|U^h\|^2_{0,\mathcal{T}_i^h}. \tag{3.5}$$

Let $R_i = R(Q_{i_1 i_2 i_3})$, then

$$\begin{aligned}(RU^h, \Pi_v(U^h))_{s_h} &= \sum_{T_i^h \in \mathcal{T}^h} (RU^h, \Pi_v(U^h))_{T_i^h} \\ &= \sum_{T_i^h \in \mathcal{T}^h} R_i(U^h, \Pi_v(U^h))_{T_i^h} + \sum_{T_i^h \in \mathcal{T}^h} ((R - R_i)U^h, \Pi_v(U^h))_{T_i^h}\end{aligned}$$

With (3.5) and Lemma 1, we clearly have

$$\sum_{T_i^h \in \mathcal{T}^h} R_i(U^h, \Pi_v(U^h))_{T_i^h} \geqslant \alpha \sum_{T_i^h \in \mathcal{T}^h} (U^h, \Pi_v(U^h))_{T_i^h} \geqslant c_5\|U^h\|^2_{L^2(\mathbf{S}^h)}, \tag{3.6}$$

and similarly we also have

$$\sum_{T_i^h \in \mathcal{T}^h} R_i(U^h, \Pi_v(U^h))_{T_i^h} \leqslant c_6\|U^h\|^2_{L^2(\mathbf{S}^h)}. \tag{3.7}$$

Since $R \in W^{1,\infty}(\mathbf{S}^h)$, it is easy to find that

$$\begin{aligned}&\left|\sum_{T_i^h \in \mathcal{T}^h} ((R - R_i)U^h, \Pi_v(U^h))_{T_i^h}\right| \leqslant \sum_{T_i^h \in \mathcal{T}^h}\sum_{j=1}^{3} |U_{i_j}^h| \int_{T_i^h \cap \mathcal{K}_{i_j}^h} |(R - R_i)U^h| d\mathbf{x} \\ &\leqslant \sum_{T_i^h \in \mathcal{T}^h} ch \sum_{j=1}^{3} |U_{i_j}^h| m(T_i^h)\left[|U_{i_j}^h| + h|\nabla_{s_h} U^h|_{T_i^h}|\right] \\ &\leqslant \sum_{T_i^h \in \mathcal{T}^h} ch \sum_{j=1}^{3} \left[|U_{i_j}^h|^2 + h|U_{i_j}^h||\nabla_{s_h} U^h|_{T_i^h}|\right] m(T_i^h) \\ &\leqslant ch\|U^h\|^2_{L^2(\mathbf{S}^h)} + ch^2\|U^h\|_{L^2(\mathbf{S}^h)}\|U^h\|_{H^1(\mathbf{S}^h)} \\ &\leqslant ch\|U^h\|^2_{L^2(\mathbf{S}^h)}\end{aligned} \tag{3.8}$$

where the last step is from the inverse inequality. The combination of (3.6), (3.7) and (3.8) deduces that

$$c_1\|U^h\|^2_{L^2(\mathbf{S}^h)} \leqslant (RU^h, \Pi_v(U^h))_{s_h} \leqslant c_2\|U^h\|^2_{L^2(\mathbf{S}^h)}$$

when h is sufficiently small and the proof is completed. □

3.5 *Existence of the finite volume solution*

Theorem 2 *The discrete problem (3.3) possesses a unique solution when h is sufficiently small.*

Proof: We only need to show that the following homogeneous system possesses solely the trivial solution:

$$\begin{cases} \mathcal{A}^h_G(U^h, \psi^h) - (\tilde{A}V^h, \psi^h)_{s_h} = 0, \\ \mathcal{A}^h_G(V^h, \phi^h) + (BU^h, \phi^h)_{s_h} = 0, \end{cases} \quad \forall \psi^h, \phi^h \in \mathcal{V}. \tag{3.9}$$

In (3.9), let $\psi^h = \Pi_v(V^h)$ and $\phi^h = \Pi_v(U^h)$ and taking the difference of the two equations, we get

$$(\tilde{A}V^h, \Pi_v(V^h))_{s_h} + (BU^h, \Pi_v(U^h))_{s_h} = 0.$$

By Lemma 4 with $r(\mathbf{x}) = \tilde{a}(\mathbf{x})$ and $r(\mathbf{x}) = b(\mathbf{x})$ respectively, and the Assumption 1, we immediately get $U^h = V^h = 0$. □

Remark 2 *If r, a and b are constant functions, then the requirement that h is sufficiently small can be removed from the conditions stated in Lemma 4 and Theorem 2.*

4. The H^1 Error Estimate

Let $\mathbf{y} = \mathbf{p}(\mathbf{x})$ and set

$$\mu_h(\mathbf{x}) = \frac{ds(\mathbf{x})}{ds_h(\mathbf{p}(\mathbf{x}))}, \quad \xi_h(\mathbf{x}) = \frac{d\gamma(\mathbf{x})}{d\gamma_h(\mathbf{p}(\mathbf{x}))}.$$

Since $\mathbf{S}$ is sufficiently smooth, when h is small enough, it is easy to find

$$|d(\mathbf{x})| \leqslant ch^2, \quad \forall \mathbf{x} \in \mathbf{S}^h,$$

for some generic constant c. Moreover, we have

$$|1 - \mu_h(\mathbf{x})| \leqslant ch^2, \quad |1 - \xi_h(\mathbf{x})| \leqslant ch^2, \quad |\vec{\mathbf{n}}(\mathbf{p}(\mathbf{x})) - \vec{\mathbf{n}}_h(\mathbf{x})| \leqslant ch.$$

It is also easy to verify

$$\nabla_{s_h} U(\mathbf{x}) = \mathbf{P}_h \nabla U(\mathbf{x}), \quad \nabla_s u(\mathbf{y}) = \mathbf{P}\nabla u(\mathbf{y}), \quad \nabla U(\mathbf{x}) = (\mathbf{P} - d\mathbf{H})\nabla u(\mathbf{y}),$$

where $\mathbf{H} = (d_{x_i,x_j}) = ((n_i)_{x_j}) = ((n_j)_{x_i})$, and $\mathbf{P}_h = (\delta_{i,j} - n_{hi}n_{hj})$ and $\mathbf{P} = (\delta_{i,j} - n_i n_j)$ are projections. Moreover, from [21], we have

$$\mathbf{PP} = \mathbf{P}, \quad \mathbf{PH} = \mathbf{HP} = \mathbf{H}, \quad \text{and} \quad \nabla_{s_h} U(\mathbf{x}) = \mathbf{P}_h(\mathbf{I} - d\mathbf{H})\nabla_s u(\mathbf{y}).$$

The following results are given in [21]:

Lemma 5 *There exist some generic constants $c_1, c_2, c_3, c_4, c_5 > 0$ such that*

$$\begin{cases} c_1\|U\|_{L^2(T_i^h)} \leqslant \|u\|_{L^2(T_i)} \leqslant c_2\|U\|_{L^2(T_i^h)}, \\ c_3\|U\|_{H^1(T_i^h)} \leqslant \|u\|_{H^1(T_i)} \leqslant c_4\|U\|_{H^1(T_i^h)}, \\ |U|_{H^2(T_i^h)} \leqslant c_5[|u|_{H^2(T_i)} + h|u|_{H^1(T_i)}] \end{cases}$$

for any $T_i \in \mathcal{T}$.

For any $u \in C^0(\mathbf{S})$, we define the interpolants $\pi_u(u)$ and $\pi_v(u)$ by

$$\pi_u(u) = \mathcal{L}(\Pi_u(\mathcal{L}^{-1}(u))), \quad \pi_v(u) = \mathcal{L}(\Pi_v(\mathcal{L}^{-1}(u))).$$

Then we have the following results (see [21, 30]):

Lemma 6 *If $u \in H^2(\mathbf{S})$, then there exist some generic constants $c_1, c_2 > 0$ such that*

$$\begin{aligned} &\|u - \pi_u(u)\|_{L^2(\mathbf{S})} + h\|u - \pi_u(u)\|_{H^1(\mathbf{S})} \leqslant c_1h^2\|u\|_{H^2(\mathbf{S})}, \\ &\|u - \pi_u(u)\|_{L^2(\mathbf{S})} \leqslant c_2h\|u\|_{H^1(\mathbf{S})}. \end{aligned}$$

For any $U^h \in \mathcal{U}$ and $\Phi^h \in \mathcal{V}$, we lift them onto $\mathbf{S}$ by $u^h = \mathcal{L}(U^h)$ and $\phi^h = \mathcal{L}(\Phi^h)$, and let

$$\psi_i^h(\mathbf{x}) = \begin{cases} 1, & \mathbf{x} \in K_i; \\ 0, & \mathbf{x} \in \mathbf{S} - K_i. \end{cases}$$

Let $\vec{\mathbf{n}}_{K_i}$ denote the outward normal of ∂K_i on K_i. For $\phi^h \in \mathcal{V}$ and $u \in H^1(\mathbf{S})$ with $u|_{T_i} \in H^2(T_i)$ for any $T_i \in \mathcal{T}$, we then define the bilinear functional $\mathcal{A}_G$ as

$$\mathcal{A}_G(u, \phi^h) = \sum_{i \in \sigma} \phi_i^h \mathcal{A}_G(u, \psi_i^h),$$

where $\phi_i^h = \phi^h(\mathbf{x}_i)$ and

$$\mathcal{A}_G(u, \psi_i^h) = -\int_{\partial K_i} \nabla_s u(\mathbf{x}) \cdot \vec{\mathbf{n}}_{K_i} d\gamma.$$

By Green's theorem, we have

$$\mathcal{A}_G(u, \psi_i^h) = -\int_{K_i} \Delta_s u \, ds \tag{4.1}$$

for any $u \in H^2(\mathbf{S})$. Consequently, if $(u, v) \in (H^2(\mathbf{S}))^2$ is the solution of the problem (2.1), then it holds that

$$\begin{cases} \mathcal{A}_G(u, \psi^h) - (\tilde{a}v, \psi^h)_s &= 0, & \forall\, \psi^h \in \mathcal{V} \\ \mathcal{A}_G(v, \phi^h) + (bu, \phi^h)_s &= (f, \phi^h)_s, & \forall\, \phi^h \in \mathcal{V}. \end{cases} \tag{4.2}$$

Lemma 7 *For any $u \in H^2(\mathbf{S})$ and $W^h \in \mathcal{U}$, there exists a generic constant $c > 0$ such that*

$$|\mathcal{A}_G^h(U, \Pi_v(W^h)) - \mathcal{A}_G^h(\Pi_u(U), \Pi_v(W^h))| \leqslant ch\|u\|_{H^2(\mathbf{S})}\|W^h\|_{H^1(\mathbf{S}^h)}, \tag{4.3}$$

$$|(BU, \Pi_v(W^h))_{s_h} - (B\Pi_u(U), \Pi_v(W^h))_{s_h}| \leqslant ch\|u\|_{H^1(\mathbf{S})}\|W^h\|_{L^2(\mathbf{S}^h)}, \tag{4.4}$$

$$|(\tilde{A}U, \Pi_v(W^h))_{s_h} - (\tilde{A}\Pi_u(U), \Pi_v(W^h))_{s_h}| \leqslant ch\|u\|_{H^1(\mathbf{S})}\|W^h\|_{L^2(\mathbf{S}^h)} \tag{4.5}$$

where $U = \mathcal{L}^{-1}(u)$.

Proof: It is easy to see that $U \in H^2(T_i^h)$ for any $T_i^h \in \mathcal{T}^h$ and $W^h \in H^1(\mathbf{S}^h)$ by Lemma 5. Let $W_i^h = W^h(\mathbf{x}_i)$ and $T_i^h = \triangle \mathbf{x}_{i_1}\mathbf{x}_{i_2}\mathbf{x}_{i_3}$ with Q_i as the centroid of T_i^h, we get

$$\begin{aligned}
\mathcal{A}_G^h(U, \Pi_v(W^h)) - \mathcal{A}_G^h(\Pi_u(U), \Pi_v(W^h)) \;&=\; \mathcal{A}_G^h(U - \Pi_u(U), \Pi_v(W^h)) \\
&= \sum_{T_i^h \in \mathcal{T}^h} \left(-\sum_{j=1}^{3} W_{i_j}^h \int_{\partial K_{i_j}^h \cap T_i^h} \nabla_{s_h}(U - \Pi_u(U)) \cdot \vec{\mathbf{n}}_{K_{i_j}^h} \, d\gamma_h \right) \\
&= \sum_{T_i^h \in \mathcal{T}^h} \left(\sum_{j=1}^{3} (W_{i_{j+2}}^h - W_{i_{j+1}}^h) \cdot \int_{\overline{M_{i_{j+1},i_{j+2}} Q_i}} \nabla_{s_h}(U - \Pi_u(U)) \cdot \vec{\mathbf{n}}_{K_{i_{j+1}}^h} \, d\gamma_h \right).
\end{aligned}$$

In each triangle T_i^h, by the mesh regularity assumption, we have

$$|W_{i_{j+2}}^h - W_{i_{j+1}}^h| \leqslant h |\nabla_{s_h} W^h|_{T_j^h}| \leqslant c \|W^h\|_{1, T_i^h}.$$

Using the trace theorem on each $K_{i_j}^h \cap T_i^h$ and the mesh regularity assumption again, we get

$$\begin{aligned}
&\left| \int_{\overline{M_{i_{j+1},i_{j+2}} Q_i}} \nabla_{s_h}(U - \Pi_u(U)) \cdot \vec{\mathbf{n}}_{K_{i_{j+1}}^h} \, d\gamma_h \right| \\
&\quad\leqslant\; c h^{1/2} \left(\int_{\overline{M_{i_{j+1},i_{j+2}} Q_i}} |\nabla_{s_h}(U - \Pi_u(U))|^2 d\gamma_h \right)^{1/2} \\
&\quad\leqslant\; c h (h^{-1} |\nabla_{s_h}(U - \Pi_u(U))|_{L^2(T_i^h)} + |\nabla_{s_h}(U - \Pi_u(U))|_{H^1(T_i^h)}) \\
&\quad\leqslant\; c h \|U\|_{H^2(T_i^h)}.
\end{aligned}$$

By Lemma 1, Lemma 5 and the Cauchy-Schwarz inequality, we then obtain

$$\begin{aligned}
|\mathcal{A}_G^h(U, \Pi_v(W^h)) - \mathcal{A}_G^h(\Pi_u(U), \Pi_v(W^h))| \;&\leqslant\; \sum_{T_i^h \in \mathcal{T}^h} c h \|U\|_{H^2(T_i^h)} \|W^h\|_{1, T_i^h} \\
&\leqslant\; c h \sum_{T_i^h \in \mathcal{T}^h} \|u\|_{H^2(T_i)} \|W^h\|_{1, T_i^h} \\
&\leqslant\; c h \|u\|_{H^2(\mathbf{S})} \|W^h\|_{H^1(\mathbf{S}^h)}
\end{aligned}$$

which gives us (4.3).

Also by Lemma 2 and Lemma 5, we get

$$\begin{aligned}
|(BU, \Pi_v(W^h))_{s_h} - (B\Pi_u(U), \Pi_v(W^h))_{s_h}| &= \left| \sum_{i \in \sigma} \int_{K_i^h} B \Pi_v(W^h)(U - \Pi_u(U)) ds_h \right| \\
&\leqslant \|B\|_{L^\infty(\mathbf{S}^h)} \int_{\mathbf{S}^h} |\Pi_v(W^h)| \cdot |U - \Pi_u(U)| ds_h \\
&\leqslant c \|b\|_{L^\infty(\mathbf{S})} \|\Pi_v(W^h)\|_{L^2(\mathbf{S}^h)} \|U - \Pi_u(U)\|_{L^2(\mathbf{S}^h)} \\
&\leqslant c h \|u\|_{H^1(\mathbf{S})} \|W^h\|_{L^2(\mathbf{S}^h)}
\end{aligned}$$

which leads to (4.4).

Applying similar analysis of (4.4) to $(\tilde{A}U, \Pi_v(W^h))_{s_h} - (\tilde{A}\Pi_u(U), \Pi_v(W^h))_{s_h}$, we get (4.5). This completes the proof. □

Lemma 8 *For any $(u, v) \in (H^2(\mathbf{S}))^2$ and $W^h \in \mathcal{U}$, there exists a generic constant $c > 0$ such that*

$$
\begin{aligned}
|\mathcal{A}_G(u, \pi_v(w^h)) - \mathcal{A}_G^h(U, \Pi_v(W^h))| &\leqslant ch\|u\|_{H^2(\mathbf{S})}\|W^h\|_{H^1(\mathbf{S}^h)}, && (4.6)\\
|(bu, \pi_v(w^h))_s - (BU, \Pi_v(W^h))_{s_h}| &\leqslant ch^2\|u\|_{L^2(\mathbf{S})}\|W^h\|_{L^2(\mathbf{S}^h)}, && (4.7)\\
|(\tilde{a}u, \pi_v(w^h))_s - (\tilde{A}U, \Pi_v(W^h))_{s_h}| &\leqslant ch^2\|u\|_{L^2(\mathbf{S})}\|W^h\|_{L^2(\mathbf{S}^h)}, && (4.8)\\
|(f, \pi_v(w^h))_s - (F, \Pi_v(W^h))_{s_h}| &\leqslant ch^2\|f\|_{L^2(\mathbf{S})}\|W^h\|_{H^1(\mathbf{S}^h)} && (4.9)
\end{aligned}
$$

where $U = \mathcal{L}^{-1}(u)$ and $w^h = \mathcal{L}(W^h)$.

Proof: It is easy to find that

$$\mathcal{A}_G(u, \pi_v(w^h)) - \mathcal{A}_G^h(U, \Pi_v(W^h)) = I_1 + I_2,$$

where

$$
\begin{aligned}
I_1 &= \sum_{i\in\sigma} -W_i^h \left(\int_{\partial K_i} \nabla_s u(\mathbf{x}) \cdot \vec{\mathbf{n}}_{K_i}(\mathbf{x}) d\gamma - \int_{\partial K_i^h} \nabla_{s_h} U(\mathbf{x}) \cdot \vec{\mathbf{n}}_{K_i}(\mathbf{p}(\mathbf{x})) d\gamma_h \right),\\
I_2 &= \sum_{i\in\sigma} -W_i^h \left(\int_{\partial K_i^h} \nabla_{s_h} U(\mathbf{x}) \cdot (\vec{\mathbf{n}}_{K_i}(\mathbf{p}(\mathbf{x})) - \vec{\mathbf{n}}_{K_i^h}(\mathbf{x})) d\gamma_h \right)
\end{aligned}
$$

For I_1, we have

$$
\begin{aligned}
I_1 &= \sum_{i\in\sigma} -W_i^h \left(\int_{\partial K_i^h} \nabla_s u(\mathbf{p}(\mathbf{x})) \cdot \vec{\mathbf{n}}_{K_i}(\mathbf{p}(\mathbf{x})) \xi_h d\gamma_h - \int_{\partial K_i^h} \nabla_{s_h} U(\mathbf{x}) \cdot \vec{\mathbf{n}}_{K_i}(\mathbf{p}(\mathbf{x})) d\gamma_h \right)\\
&= \sum_{i\in\sigma} -W_i^h \int_{\partial K_i^h} (\xi_h \nabla_s u(\mathbf{p}(\mathbf{x})) - \nabla_{s_h} U(\mathbf{x})) \cdot \vec{\mathbf{n}}_{K_i}(\mathbf{p}(\mathbf{x})) d\gamma_h\\
&= \sum_{T_i\in\mathcal{T}} \left(-\sum_{j=1}^{3} W_{i_j}^h \int_{\partial K_i^h \cap T_i^h} (\xi_h \nabla_s u(\mathbf{p}(\mathbf{x})) - \nabla_{s_h} U(\mathbf{x})) \cdot \vec{\mathbf{n}}_{K_i}(\mathbf{p}(\mathbf{x})) d\gamma_h \right)\\
&= \sum_{T_i^h\in\mathcal{T}^h} \left(\sum_{j=1}^{3} (W_{i_{j+2}}^h - W_{i_{j+1}}^h) \cdot \int_{\overline{M_{i_{j+1}, i_{j+2}} Q_i}} (\xi_h \nabla_s u(\mathbf{p}(\mathbf{x})) - \nabla_{s_h} U(\mathbf{x})) \cdot \vec{\mathbf{n}}_{K_{i_{j+1}}^h} d\gamma_h \right).
\end{aligned}
$$

For I_2, we rewrite it as

$$
I_2 = \sum_{T_i^h\in\mathcal{T}^h} \left(\sum_{j=1}^{3} (W_{i_{j+2}}^h - W_{i_{j+1}}^h) \cdot \int_{\overline{M_{i_{j+1}, i_{j+2}} Q_i}} \nabla_{s_h} U \cdot (\vec{\mathbf{n}}_{K_{i_{j+1}}}(\mathbf{p}(\mathbf{x})) - \vec{\mathbf{n}}_{K_{i_{j+1}}^h}(\mathbf{x})) d\gamma_h \right)
$$

Since $|\vec{\mathbf{n}}_{K_i}(\mathbf{p}(\mathbf{x})) - \vec{\mathbf{n}}_{K_i^h}(\mathbf{x})| \leqslant ch$, by Lemma 1, Lemma 5 and the trace theorem, we obtain that,

$$\begin{aligned} |I_2| &\leqslant \sum_{T_i^h \in \mathcal{T}^h} ch\|W^h\|_{1,T_i^h}\|U\|_{H^2(T_i^h)} \\ &\leqslant ch \sum_{T_i^h \in \mathcal{T}^h} \|u\|_{H^2(T_i)}\|W^h\|_{1,T_i^h} \\ &\leqslant ch\|u\|_{H^2(\mathbf{S})}\|W^h\|_{H^1(\mathbf{S}^h)}. \end{aligned} \tag{4.10}$$

We observe that

$$\begin{aligned} \xi_h \nabla_s u(\mathbf{p}(\mathbf{x})) - \nabla_{s_h} U(\mathbf{x}) &= (\xi_h \mathbf{I} - \mathbf{P}_h(\mathbf{I} - d\mathbf{H}))\mathbf{P}\nabla_s u(\mathbf{p}(\mathbf{x})) \\ &= \xi_h(\mathbf{P} - \frac{1}{\xi_h}\mathbf{P}_h(\mathbf{I} - d\mathbf{H})\mathbf{P})\nabla_s u(\mathbf{p}(\mathbf{x})). \end{aligned}$$

Since $|1 - \xi_h| < ch^2$, we have for h small that

$$\begin{aligned} |\xi_h(\mathbf{P} - \frac{1}{\xi_h}\mathbf{P}_h(\mathbf{I} - d\mathbf{H})\mathbf{P})| &\leqslant |\mathbf{P} - \mathbf{P}_h(\mathbf{I} - d\mathbf{H})\mathbf{P}| + ch^2 \\ &\leqslant |\mathbf{P} - \mathbf{P}_h\mathbf{P}| + ch^2 \\ &\leqslant ch + ch^2 \\ &\leqslant ch. \end{aligned}$$

So we know

$$|\xi_h \nabla_s u(\mathbf{p}(\mathbf{x})) - \nabla_{s_h} U(\mathbf{x})| \leqslant ch|\nabla_s u(\mathbf{p}(\mathbf{x}))| \leqslant ch|\nabla_{s_h} U(\mathbf{x})|.$$

Then using similar analysis as for I_2, we can show that

$$|I_1| \leqslant ch\|u\|_{H^2(\mathbf{S})}\|W^h\|_{H^1(\mathbf{S}^h)}. \tag{4.11}$$

Combining (4.11) with (4.10), we get the first estimate (4.6). Notice that

$$\begin{aligned} |(bu, \pi_v(w^h))_s - (BU, \mathit{\Pi}_v(W^h))_{s_h}| &= \left|\int_{\mathbf{S}} bu\pi_v(w^h)ds - \int_{\mathbf{S}_h} BU\mathit{\Pi}_v(W^h)ds_h\right| \\ &= \left|\int_{\mathbf{S}^h} BU\mathit{\Pi}_v(W^h)\mu_h ds_h - \int_{\mathbf{S}^h} BU\mathit{\Pi}_v(W^h)ds_h\right| \\ &= \left|\int_{\mathbf{S}^h} (1-\mu_h)BU\mathit{\Pi}_v(W^h)ds_h\right| \\ &\leqslant ch^2\|b\|_{L^\infty(\mathbf{S})}\|U\|_{L^2(\mathbf{S}^h)}\|W^h\|_{L^2(\mathbf{S}^h)} \\ &\leqslant ch^2\|u\|_{L^2(\mathbf{S})}\|W^h\|_{L^2(\mathbf{S}^h)}\ , \end{aligned}$$

we get the second estimate (4.7). Using similar analysis as the above, we also can get (4.8).

Finally, we have

$$\begin{aligned}|(f,\pi_v(w^h))_s-(F,\Pi_v(W^h))_{s_h}| &= \left|\int_{\mathbf{S}} f(\mathbf{x})\pi_v(w^h)(\mathbf{x})ds-\int_{\mathbf{S}^h} F(\mathbf{x})\Pi_v(W^h)(\mathbf{x})ds_h\right| \\ &= \left|\int_{\mathbf{S}^h}(1-\mu_h)F\Pi_v(W^h)ds_h\right| \\ &\leqslant ch^2\|F\|_{L^2(\mathbf{S}^h)}\|W^h\|_{L^2(\mathbf{S}^h)} \\ &\leqslant ch^2\|f\|_{L^2(\mathbf{S})}\|W^h\|_{L^2(\mathbf{S}^h)}\end{aligned}$$

This gives us (4.9). □

Lemma 9 *Suppose that $(u,v)\in(H^2(\mathbf{S}))^2$ is the solution of the problem (2.1), and $(U^h,V^h)\in\mathcal{U}\times\mathcal{U}$ is the solution of the discrete problem (3.3). Let $U=\mathcal{L}^{-1}(u)$, $V=\mathcal{L}^{-1}(v)$, then there exists some generic constant $c>0$ such that*

$$\begin{aligned}&\|U^h-\Pi_u(U)\|^2_{L^2(\mathbf{S}^h)}+\|V^h-\Pi_u(V)\|^2_{L^2(\mathbf{S}^h)} \\ &\quad\leqslant ch\|f\|_{L^2(\mathbf{S})}\left[\|U^h-\Pi_u(U)\|_{H^1(\mathbf{S}^h)}+\|V^h-\Pi_u(V)\|_{H^1(\mathbf{S}^h)}\right].\end{aligned}\tag{4.12}$$

Proof: For any $W^h\in\mathcal{U}$, let $w^h=\mathcal{L}(W^h)$. By Lemmas 7 and 8, it holds that

$$\begin{aligned}&|\mathcal{A}^h_G(\Pi_u(U),\Pi_v(W^h))-\mathcal{A}_G(u,\pi_v(w^h))| \\ &\quad\leqslant|\mathcal{A}^h_G(\Pi_u(U),\Pi_v(W^h))-\mathcal{A}^h_G(U,\Pi_v(W^h))|+|\mathcal{A}^h_G(U,\Pi_v(W^h))-\mathcal{A}_G(u,\pi_v(w^h))| \\ &\quad\leqslant ch\|u\|_{H^2(\mathbf{S})}\|W^h\|_{H^1(\mathbf{S}^h)}\end{aligned}\tag{4.13}$$

and

$$\begin{aligned}&|(\Pi_u(\tilde{A}V),\Pi_v(W^h))_{s_h}-(\tilde{a}v,\pi_v(w^h))_s| \\ &\quad\leqslant|(\Pi_u(\tilde{A}V),\Pi_v(W^h))_{s_h}-(\tilde{A}V,\Pi_v(W^h))_{s_h}|+|\tilde{A}V,\Pi_v(W^h)_{s_h}-(\tilde{a}v,\pi_v(w^h))_s| \\ &\quad\leqslant ch\|\tilde{A}V\|_{H^1(\mathbf{S}^h)}\|W^h\|_{L^2(\mathbf{S}^h)}+ch\|\tilde{a}v\|_{H^1(\mathbf{S})}\|W^h\|_{L^2(\mathbf{S}^h)} \\ &\quad\leqslant ch\|v\|_{H^1(\mathbf{S})}\|W^h\|_{L^2(\mathbf{S}^h)}\end{aligned}\tag{4.14}$$

since $\tilde{a}\in W^{2,\infty}(\mathbf{S})$. Moreover,

$$\begin{aligned}&|(\Pi_u(\tilde{A}V),\Pi_v(W^h))_{s_h}-(\tilde{A}\Pi_u(V),\Pi_v(W^h))_{s_h}| \\ &\quad=|(\Pi_u(\tilde{A}V),\Pi_v(W^h))_{s_h}-(\tilde{A}V,\Pi_v(W^h))_{s_h}| \\ &\qquad\quad+|(\tilde{A}V,\Pi_v(W^h))_{s_h}-(\tilde{A}\Pi_u(V),\Pi_v(W^h))_{s_h}| \\ &\quad\leqslant\|\tilde{A}V-\Pi_u(\tilde{A}V)\|_{L^2(\mathbf{S}^h)}\|W^h\|_{L^2(\mathbf{S}^h)}+ch\|v\|_{H^1(\mathbf{S})}\|W^h\|_{L^2(\mathbf{S}^h)} \\ &\quad\leqslant ch\|v\|_{H^1(\mathbf{S})}\|W^h\|_{L^2(\mathbf{S}^h)}.\end{aligned}\tag{4.15}$$

The combination of (4.14) and (4.15) leads to

$$|(\tilde{A}\Pi_u(V),\Pi_v(W^h))_{s_h}-(\tilde{a}v,\pi_v(w^h))_s|\leqslant ch\|v\|_{H^1(\mathbf{S})}\|W^h\|_{L^2(\mathbf{S}^h)}.\tag{4.16}$$

By (4.2), it is easy to find that (u,v) satisfies

$$\mathcal{A}_G(u,\pi_v(w^h))-(\tilde{a}v,\pi_v(w^h))_s=0.\tag{4.17}$$

Putting (4.13) and (4.16) into (4.17), we get

$$|\mathcal{A}_G^h(\Pi_u(U),\Pi_v(W^h)) - (\tilde{A}\Pi_u(V),\Pi_v(W^h))_{s_h}| \leqslant ch(\|u\|_{H^2(\mathbf{S})} + \|v\|_{H^1(\mathbf{S})})\|W^h\|_{H^1(\mathbf{S}^h)}.$$

Using the estimate (2.3), we get

$$|\mathcal{A}_G^h(\Pi_u(U),\Pi_v(W^h)) - (\tilde{A}\Pi_u(V),\Pi_v(W^h))_{s_h}| \leqslant ch\|f\|_{L^2(\mathbf{S})}\|W^h\|_{H^1(\mathbf{S}^h)}. \tag{4.18}$$

Subtracting the first equation in (3.3) (letting $\psi^h = \Pi_v(W^h)$) from (4.18), we obtain

$$\begin{aligned}&\mathcal{A}_G^h(\Pi_u(U) - U^h,\Pi_v(W^h)) - (\tilde{A}(\Pi_u(V) - V^h),\Pi_v(W^h))_{s_h}\\ &\quad\leqslant ch(\|u\|_{H^2(\mathbf{S})} + \|v\|_{H^1(\mathbf{S})})\|W^h\|_{H^1(\mathbf{S}^h)} \leqslant ch\|f\|_{L^2(\mathbf{S})}\|W^h\|_{H^1(\mathbf{S}^h)}\,.\end{aligned} \tag{4.19}$$

At the same time, we note that

$$\mathcal{A}_G(v,\pi_v(w^h)) + (bu,\pi_v(w^h))_s = (f,\pi_v(w^h))_s, \tag{4.20}$$

and

$$\mathcal{A}_G^h(V^h,\Pi_v(W^h)) + (BU^h,\Pi_v(W^h))_{s_h} = (F,\Pi_v(W^h))_{s_h}. \tag{4.21}$$

Using similar techniques as in the above, and noticing the difference between $(f,\pi_v(w^h))_s$ and $(F,\Pi_v(W^h))_{s_h}$ given in Lemma 8, we can easily get

$$\begin{aligned}&\mathcal{A}_G^h(\Pi_u(V) - V^h,\Pi_v(W^h)) + (B(\Pi_u(U) - U^h),\Pi_v(W^h))_{s_h}\\ &\quad\leqslant ch(\|u\|_{H^1(\mathbf{S})} + \|v\|_{H^2(\mathbf{S})})\|W^h\|_{H^1(\mathbf{S}^h)} \leqslant ch\|f\|_{L^2(\mathbf{S})}\|W^h\|_{H^1(\mathbf{S}^h)}\,.\end{aligned} \tag{4.22}$$

Now let us set $W^h = V^h - \Pi_u(V)$ in (4.19) and $W^h = \Pi_u(U) - U^h$ in (4.22) and add them together. By the symmetry of $\mathcal{A}_G^h(\cdot,\Pi_v(\cdot))$ shown in Lemma 3, after reordering, we obtain the left-hand side of the above sum as

$$\begin{aligned}\text{LHS} &= \left[\mathcal{A}_G^h(\Pi_u(U) - U^h,\Pi_v(V^h - \Pi_u(V))) + \mathcal{A}_G^h(\Pi_u(V) - V^h,\Pi_v(\Pi_u(U) - U^h))\right]\\ &\quad + \left[-(\tilde{A}(\Pi_u(V) - V^h),\Pi_v(V^h - \Pi_u(V)))_{s_h} + (B(\Pi_u(U) - U^h),\Pi_v(\Pi_u(U) - U^h))_{s_h}\right]\\ &= \left[-\mathcal{A}_G^h(\Pi_u(U) - U^h,\Pi_v(\Pi_u(V) - V^h)) + \mathcal{A}_G^h(\Pi_u(V) - V^h,\Pi_v(\Pi_u(U) - U^h))\right]\\ &\quad + \left[(\tilde{A}(V^h - \Pi_u(V)),\Pi_v(V^h - \Pi_u(V)))_{s_h} + (B(\Pi_u(U) - U^h),\Pi_v(\Pi_u(U) - U^h))_{s_h}\right]\\ &= (\tilde{A}(V^h - \Pi_u(V)),\Pi_v(V^h - \Pi_u(V)))_{s_h} + (B(\Pi_u(U) - U^h),\Pi_v(\Pi_u(U) - U^h))_{s_h}.\end{aligned}$$

Hence, by the inequalities (4.19) and (4.22), we get

$$\begin{aligned}&(\tilde{A}(V^h - \Pi_u(V)),\Pi_v(V^h - \Pi_u(V)))_{s_h} + (B(U^h - \Pi_u(U)),\Pi_v(U^h - \Pi_u(U)))_{s_h}\\ &\quad\leqslant\ ch(\|u\|_{H^2(\mathbf{S})} + \|v\|_{H^2(\mathbf{S})})\left[\|U^h - \Pi_u(U)\|_{H^1(\mathbf{S}^h)} + \|V^h - \Pi_u(V)\|_{H^1(\mathbf{S}^h)}\right]\\ &\quad\leqslant\ ch\|f\|_{L^2(\mathbf{S})}\left[\|U^h - \Pi_u(U)\|_{H^1(\mathbf{S}^h)} + \|V^h - \Pi_u(V)\|_{H^1(\mathbf{S}^h)}\right]\,.\end{aligned} \tag{4.23}$$

Notice that $U^h - \Pi_u(U), V^h - \Pi_u(V) \in \mathcal{U}$, using Assumption 1 and Lemma 4, it is then easy to deduce (4.12) from (4.23) and the proof is thus completed. □

Theorem 3 *Suppose that $(u,v)\in (H^2(\mathbf{S}))^2$ is the solution of the problem (2.1), and $(U^h,V^h)\in \mathcal{U}\times\mathcal{U}$ is the solution of the discrete problem (3.3). Let $u^h=\mathcal{L}(U^h)$ and $v^h=\mathcal{L}(V^h)$, then there exists some generic constant $c>0$ such that*

$$\|u-u^h\|_{H^1(\mathbf{S})}+\|v-v^h\|_{H^1(\mathbf{S})}\leqslant ch\|f\|_{L^2(\mathbf{S})}\,. \tag{4.24}$$

Proof: We extend u,v onto $\mathbf{S}^h$ by $U=\mathcal{L}^{-1}(u)$ and $V=\mathcal{L}^{-1}(v)$. By Proposition 1, we have

$$\begin{aligned}&|U^h-\Pi_u(U)|^2_{H^1(\mathbf{S}^h)}+|V^h-\Pi_u(V)|^2_{H^1(\mathbf{S}^h)}\\&\quad=\mathcal{A}^h_G(U^h-\Pi_u(U),\Pi_v(U^h-\Pi_u(U)))+\mathcal{A}^h_G(V^h-\Pi_u(V),\Pi_v(V^h-\Pi_u(V))).\end{aligned}$$

Setting $W^h=\Pi_u(U)-U^h$ in (4.19) and $W^h=\Pi_u(V)-V^h$ in (4.22), adding them up and putting back into the above equality, we then obtain that

$$\begin{aligned}&|U^h-\Pi_u(U)|^2_{H^1(\mathbf{S}^h)}+|V^h-\Pi_u(V)|^2_{H^1(\mathbf{S}^h)}\\&\leqslant\ |(\tilde{A}(\Pi_u(V)-V^h),\Pi_v(\Pi_u(U)-U^h))_{s_h}|+|(B(\Pi_u(U)-U^h),\Pi_v(\Pi_u(V)-V^h))_{s_h}|\\&\quad+ch(\|u\|_{H^2(\mathbf{S})}+\|v\|_{H^2(\mathbf{S})})\left[\|U^h-\Pi_u(U)\|_{H^1(\mathbf{S}^h)}+\|V^h-\Pi_u(V)\|_{H^1(\mathbf{S}^h)}\right]\\&\leqslant\ c(\|U^h-\Pi_u(U)\|^2_{L^2(\mathbf{S}^h)}+\|V^h-\Pi_u(V)\|^2_{L^2(\mathbf{S}^h)})\\&\quad+ch(\|u\|_{H^2(\mathbf{S})}+\|v\|_{H^2(\mathbf{S})})\left[\|U^h-\Pi_u(U)\|_{H^1(\mathbf{S}^h)}+\|V^h-\Pi_u(V)\|_{H^1(\mathbf{S}^h)}\right]\\&\leqslant\ ch(\|u\|_{H^2(\mathbf{S})}+\|v\|_{H^2(\mathbf{S})})\left[\|U^h-\Pi_u(U)\|_{H^1(\mathbf{S}^h)}+\|V^h-\Pi_u(V)\|_{H^1(\mathbf{S}^h)}\right]\end{aligned}\tag{4.25}$$

where the last inequality is due to Lemma 9.

The sum of (4.25) and (4.12) gives us

$$\begin{aligned}&\|U^h-\Pi_u(U)\|^2_{H^1(\mathbf{S}^h)}+\|V^h-\Pi_u(V)\|^2_{H^1(\mathbf{S}^h)}\\&\qquad\leqslant\ ch(\|u\|_{H^2(\mathbf{S})}+\|v\|_{H^2(\mathbf{S})})\left[\|U^h-\Pi_u(U)\|_{H^1(\mathbf{S}^h)}+\|V^h-\Pi_u(V)\|_{H^1(\mathbf{S}^h)}\right],\end{aligned}$$

and consequently, by using (2.3), we get

$$\|U^h-\Pi_u(U)\|_{H^1(\mathbf{S}^h)}+\|V^h-\Pi_u(V)\|_{H^1(\mathbf{S}^h)}\leqslant ch(\|u\|_{H^2(\mathbf{S})}+\|v\|_{H^2(\mathbf{S})})\leqslant ch\|f\|_{L^2(\mathbf{S})}\,. \tag{4.26}$$

In addition, by Lemmas 5 and 6, we have

$$\|U-\Pi_u(U)\|_{H^1(\mathbf{S}^h)}\leqslant c\|u-\pi_u(u)\|_{H^1(\mathbf{S})}\leqslant ch\|u\|_{H^2(\mathbf{S})}, \tag{4.27}$$

$$\|V-\Pi_u(V)\|_{H^1(\mathbf{S}^h)}\leqslant c\|v-\pi_u(v)\|_{H^1(\mathbf{S})}\leqslant ch\|v\|_{H^2(\mathbf{S})}. \tag{4.28}$$

Combining (4.26)-(4.28), we finally obtain

$$\begin{aligned}\|u-u^h\|_{H^1(\mathbf{S})}+\|v-v^h\|_{H^1(\mathbf{S})}&\leqslant c\left(\|U-U^h\|_{H^1(\mathbf{S}^h)}+\|V-V^h\|_{H^1(\mathbf{S}^h)}\right)\\&\leqslant c\left(\|U^h-\Pi_u(U)\|_{H^1(\mathbf{S}^h)}+\|U-\Pi_u(U)\|_{H^1(\mathbf{S}^h)}\right.\\&\qquad\left.+\|V^h-\Pi_u(V)\|_{H^1(\mathbf{S}^h)}+\|V-\Pi_u(V)\|_{H^1(\mathbf{S}^h)}\right)\\&\leqslant ch\|f\|_{L^2(\mathbf{S})}\,.\end{aligned}$$

This completes the proof. □

5. Quality Surface Meshes and Gradient Recovery

The design of a sequence of high-quality surface triangulations (satisfying mesh regularity requirement) with increasing levels of resolutions is a challenging research subject in its own right. To ensure the accurate finite volume solution, we now discuss a possible approach for obtaining regular and smooth meshes. The meshes of the surface $\mathbf{S}$ to be used in our numerical experiments for the discretization of PDEs on surfaces are generated by the so-called constrained centroidal Voronoi Delaunay triangulation (CCVDT) algorithm [17]. We now give a brief description below.

Given a density function $\rho(\mathbf{x})$ defined on $\mathbf{S}$, for any region $V \subset \mathbf{S}$, we call $\mathbf{x}^c$ the *constrained mass centroid of* V *on* $\mathbf{S}$ if

$$\mathbf{x}^c = \arg\min_{\mathbf{x}\in V} F(\mathbf{x})\,, \qquad \text{where} \qquad F(\mathbf{x}) = \int_V \rho(\mathbf{y})\|\mathbf{y}-\mathbf{x}\|^2\, ds(\mathbf{y})\,. \tag{5.1}$$

The existence of solutions of (5.1) can be easily obtained by using the continuity and compactness of F; however, solutions may not be unique. In general, given a Voronoi tessellation $\mathcal{W} = \{\mathbf{x}_i, V_i\}_{i=1}^n$ of $\mathbf{S}$, the generators $\{\mathbf{x}_i\}_{i=1}^n$ do not coincide with $\{\mathbf{x}_i^c\}_{i=1}^n$, where $\mathbf{x}_i^c$ denotes the constrained mass centroid of V_i for $i = 1, \ldots, n$. We refer to a Voronoi tessellation of $\mathbf{S}$ as a *constrained centroidal Voronoi tessellation* (CCVT) if and only if the points $\{\mathbf{x}_i\}_{i=1}^n$ which serve as the generators of the associated Voronoi tessellation $\{V_i\}_{i=1}^n$ are also the constrained mass centroids of those regions [17], i.e., if and only if we have that

$$\mathbf{x}_i = \mathbf{x}_i^c \quad \text{for } i = 1, \ldots, n\,.$$

The CCVT is a generalization of the standard CVT [16] which is a concept with many applications including mesh generation and optimization. The dual tessellation of CCVT of $\mathbf{S}$ is then called a *constrained centroidal Voronoi Delaunay triangulation* (CCVDT). Constrained centroidal Voronoi meshes on surfaces in $\mathbb{R}^3$ have many good geometric properties, see [17, 20] for detailed studies as well as efficient algorithms for constructing CCVT/CCVDT meshes.

For a constant density function, the generators $\{\mathbf{x}_i\}_{i=1}^n$ are uniformly distributed in some sense; the V_i's are all almost of the same size and most of them are similar convex surface hexagons; the mesh size h is approximately proportional to $1/\sqrt{n}$. For a non-constant density function, the generators $\{\mathbf{x}_i\}_{i=1}^n$ are still locally uniformly distributed and it is conjectured that, asymptotically, $h_i/h_j \approx (\rho(\mathbf{x}_j)/\rho(\mathbf{x}_i))^{1/4}$. This property of local quasi-uniformity of CCVDT meshes gives us an excellent chance to recover the approximation of $\nabla_s u$ and $\nabla_s v$ in high order based on the $\nabla_{s_h} U^h$ and $\nabla_{s_h} V^h$.

Let us take a simple averaging scheme similar to the one suggested in [18]. For any vertex $\mathbf{x}_i$, let $D_i = \{T_j^h \mid \mathcal{T}_j^h \in \mathcal{T}^h, \mathbf{x}_i \in T_j^h\}$, then set

$$DU(\mathbf{x}_i) = \frac{1}{\mathrm{Card}(D_i)}\Big(\sum_{T_j^h\in D_i} \nabla_{s_h} U|_{T_j^h}\Big)\,, \quad DV(\mathbf{x}_i) = \frac{1}{\mathrm{Card}(D_i)}\Big(\sum_{T_j^h\in D_i} \nabla_{s_h} V|_{T_j^h}\Big).$$

Now let the vector-valued functions DU^h and DV^h be the corresponding piecewise defined functions on $\mathbf{S}^h$ that interpolate $\{DU(\mathbf{x}_i)\}_{i=1}^n$ and $\{DV(\mathbf{x}_i)\}_{i=1}^n$ respectively. We also use $Du^h = \mathcal{L}(DU^h)$ and $Dv^h = \mathcal{L}(DV^h)$ as the new approximations to the surface gradients $\nabla_s u$ and $\nabla_s v$ respectively. We expect that this averaging scheme with the underlying CCVDT

mesh on $\mathbf{S}$ gives second order approximations to $\nabla_s u$ and $\nabla_s v$ in L^2 norm and first order approximations in H^1 norm. Then the same averaging scheme can be applied to Du^h and Dv^h to recover more accurately the tensors $\nabla_s(\nabla_s u)$ and $\nabla_s(\nabla_s v)$ respectively. A numerical demonstration of this superconvergent recovery is given in the later numerical experiments.

6. Numerical Experiments

To illustrate the finite volume method proposed and analyzed in the paper and to validate the sharpness of the convergence rates proved in the previous sections, numerical experiments are performed for some model geometries with some given exact solutions of equation (1.1). The simple mass-lumped scheme (3.4) is used in the practical implementation.

Let n_i denote the number of nodes of the mesh at the ith level and $u^{h,i}$ the corresponding discrete solution, we calculate the convergence rate CR with respect to the norm $\|\cdot\|$ by

$$\mathrm{CR} = \frac{2\log(\|u-u^{h,i}\|/\|u-u^{h,i-1}\|)}{\log(n_{i-1}/n_i)}.$$

Example 1 *The surface* $\mathbf{S}$ *is chosen to be the unit sphere* $\mathbf{S} = \{\mathbf{x} \in \mathbb{R}^3 \mid x_1^2 + x_2^2 + x_3^2 = 1\}$, *and the outward normal at* $\mathbf{x} \in \mathbf{S}$ *is given by* $\vec{\mathbf{n}}(\mathbf{x}) = \mathbf{x}/\|\mathbf{x}\|$. *Let the coefficients in the equation (1.1) be given by* $a(\mathbf{x}) = 1 + 3x_1^2$ *and* $b(\mathbf{x}) = 1 + x_3^2$. *The exact solution is chosen to be* $u(\mathbf{x}) = 10x_1x_2x_3(x_1^2 - x_2^2)$ *and consequently*

$$v(\mathbf{x}) = -a(\mathbf{x})\Delta_s u(\mathbf{x}) = 300x_1x_2x_3(x_1^2 - x_2^2)(1 + 3x_2^2)/(x_1^2 + x_2^2 + x_3^2).$$

The right hand side $f(\mathbf{x})$ *is set correspondingly from (1.1). We note that the norms of the exact solution are* $\|u\|_{L^2(\mathbf{S})} \approx 1.2024e+00$, $\|u\|_{H^1(\mathbf{S})} \approx 3.6698e+01$, $\|u\|_{H^2(\mathbf{S})} \approx 3.6698e+01$, *and* $\|v\|_{L^2(\mathbf{S})} \approx 8.3729e+01$, $\|v\|_{H^1(\mathbf{S})} \approx 4.7398e+02$, $\|v\|_{H^2(\mathbf{S})} \approx 2.7276e+03$, *respectively.*

Applying the finite volume method discussed in the paper to solve the Example 1, we adopt some CCVDT meshes with a uniform density function and five different levels of resolution, that is, n_i is taken to be 104, 410, 1634, 6530, and 26114 respectively. Let h_{max} denote the largest diameter of the surface mesh, then the corresponding h_{max} for each mesh level is 0.5973, 0.3194, 0.1705, 0.0887 and 0.0457, respectively. The computational results are reported in Table 1. Some meshes and corresponding discrete solutions are also plotted in Figure 2, with the variations in colors representing the different values of the numerical solution. The convergence rate is obviously consistent to our theoretical analysis and the errors for both u and v are about the same order when taking into account the difference in their respective norms. The gradient recovery scheme for the first order derivatives is also seen to give an extra order of accuracy. For the second order derivatives, the convergence rate is expected to be at least linear, but the computation shows that the rate behaves nearly to be second order, see Table 2.

Example 2 *Now we let the surface* $\mathbf{S}$ *be an ellipse defined by* $\mathbf{S} = \{\mathbf{x} \in \mathbb{R}^3 \mid x_1^2 + x_2^2 + x_3^2/4 = 1\}$ *and the outward normal at* $\mathbf{x} \in \mathbf{S}$ *is given by* $\vec{\mathbf{n}}(\mathbf{x}) = \vec{t}/|\vec{t}|$ *with* $\vec{t} = (x_1, x_2, x_3/4)$. *The coefficients in the equation (1.1) are given by* $a(\mathbf{x}) = 1 + x_3^2$ *and* $b(\mathbf{x}) = 1$. *An exact solution is chosen to be* $u(\mathbf{x}) = e^{x_3-2}$ *with the corresponding*

$$v(\mathbf{x}) = 8(1 + x_3^2)e^{x_3-2}\frac{(32x_1^4 + 64x_1^2x_2^2 + 2x_1^2x_3^2 - 10x_1^2x_3 - x_3^3 - 10x_3x_2^2 + 2x_2^2x_3^2 + 32x_2^4)}{(16x_1^2 + 16x_2^2 + x_3^2)^2}.$$

Table 1. Computational results on CCVDT meshes for Example 1.

Nodes	$\|u-u^h\|_{L^\infty}$	CR	$\|u-u^h\|_{L^2}$	CR	$\|u-u^h\|_{H^1}$	CR
104	2.8433e-01	-	2.5018e-01	-	3.8341e+00	-
410	7.4405e-02	1.95	5.6339e-02	2.17	1.7396e+00	1.15
1634	2.6583e-02	1.48	1.5414e-02	1.87	8.5407e-01	1.03
6530	5.3530e-03	2.31	4.0513e-03	1.93	4.2474e-01	1.01
26114	1.7167e-03	1.64	1.1581e-03	1.81	2.1211e-01	1.00
Nodes	$\|v-v^h\|_{L^\infty}$	CR	$\|v-v^h\|_{L^2}$	CR	$\|v-v^h\|_{H^1}$	CR
104	1.5978e+01	-	1.7780e+01	-	2.2675e+02	-
410	4.8971e+00	1.72	4.7457e+00	1.93	1.2229e+02	0.90
1634	1.2964e+00	1.92	1.2064e+00	1.98	6.2249e+01	0.98
6530	3.3235e-01	1.97	3.0247e-01	2.00	3.1257e+01	0.99
26114	9.0692e-02	1.88	7.5731e-02	2.00	6.6842e+00	1.00

Table 2. Errors after gradient recovery on CCVDT meshes for Example 1.

Nodes	$\|\nabla_s u - Du^h\|_{L^2}$	CR	$\|\nabla_s u - Du^h\|_{H^1}$	CR	$\|\nabla_s(\nabla_s u) - D(Du^h)\|_{L^2}$	CR
104	2.8350e+00	-	1.6286e+01	-	2.4111e+01	-
410	9.2057e-01	1.64	6.8778e+00	1.26	1.0214e+01	1.25
1634	2.4568e-01	1.91	3.1216e+00	1.14	2.9765e+00	1.78
6530	6.2847e-02	1.97	1.5102e+00	1.05	7.9906e-01	1.90
26114	1.5958e-02	1.98	7.4858e-01	1.01	2.2469e-01	1.83
Nodes	$\|\nabla_s v - Dv^h\|_{L^2}$	CR	$\|\nabla_s v - Dv^h\|_{H^1}$	CR	$\|\nabla_s(\nabla_s v) - D(Dv^h)\|_{L^2}$	CR
104	2.6002e+02	-	1.5469e+03	-	2.0428e+03	-
410	9.4464e+01	1.48	6.4426e+02	1.28	9.5499e+02	1.11
1634	2.6031e+01	1.86	2.6645e+02	1.28	2.8956e+02	1.73
6530	6.6842e+00	1.96	1.2310e+02	1.11	7.7510e+01	1.90
26114	1.6880e+00	1.99	6.0144e+01	1.04	2.0918e+01	1.89

The right hand side $f(\mathbf{x})$ is again set correspondingly from (1.1). We note that the norms of the exact solution are $\|u\|_{L^2(\mathbf{S})} \approx 1.4988e+00$, $\|u\|_{H^1(\mathbf{S})} \approx 6.6966e+00$, $\|u\|_{H^2(\mathbf{S})} \approx 3.6698e+01$, and $\|v\|_{L^2(\mathbf{S})} \approx 8.3729e+01$, $\|v\|_{H^1(\mathbf{S})} \approx 4.7398e+02$, $\|v\|_{H^2(\mathbf{S})} \approx 2.7276e+03$, respectively.

The Example 2 is also numerically solved by the finite volume method studied here on five levels of CCVDT meshes with number of nodes n_i=147, 582, 2322, 9282 and 37122, respectively. We choose a nonuniform density $\rho(\mathbf{x}) = e^{x_3-2}+0.01$ for the CCVDT mesh construction in order to better capture the variations of u on the surface. The constant 0.01 is used in ρ to further regularize the resulting CCVDT mesh. The corresponding h_{max} for each mesh level is 0.8983, 0.5559, 0.2781, 0.1464, and 0.0768 respectively. The computational results are reported in Tables 3 and 4. The meshes and corresponding discrete solutions are plotted in Figure 3. The numerical accuracies of the solution, the recovered gradients and the recovered high order derivatives are again consistent to that predicted by the analysis.

Although our analysis in the former sections is only for the case $\partial\mathbf{S} = \emptyset$, here we still use an example to test the performance of the proposed mixed finite volume discretization for the

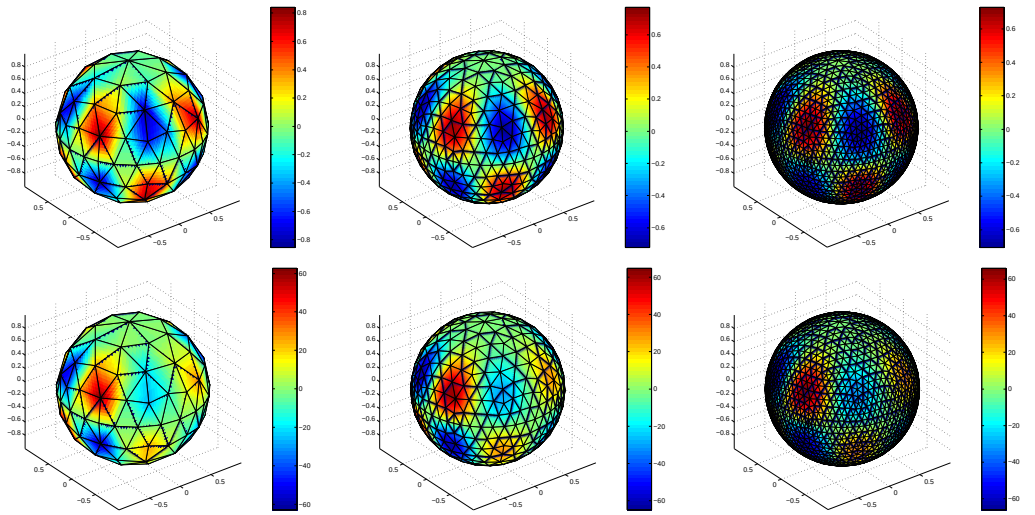

FIG. 2. Discrete solution u^h (top line) and v^h (bottom line) for Example 1 with $104, 410, 1634$ nodes respectively.

Table 3. Computational results on CCVDT meshes for Example 2.

Nodes	$\|u-u^h\|_{L^\infty}$	CR	$\|u-u^h\|_{L^2}$	CR	$\|u-u^h\|_{H^1}$	CR
147	7.8792e-02	-	2.1097e-01	-	2.7687e-01	-
582	1.0458e-02	2.94	3.6830e-02	2.54	8.0801e-02	1.79
2322	3.2891e-03	1.67	7.1222e-03	2.37	3.5877e-02	1.17
9282	1.0273e-03	2.68	1.9201e-03	1.89	1.7635e-02	1.03
37122	1.8440e-04	2.48	3.1217e-04	2.62	8.7463e-03	1.01
Nodes	$\|v-v^h\|_{L^\infty}$	CR	$\|v-v^h\|_{L^2}$	CR	$\|v-v^h\|_{H^1}$	CR
147	3.1860e+00	-	8.0644e-01	-	1.1734e+01	-
582	5.4774e-01	2.56	1.3844e-01	2.56	4.8611e+00	1.28
2322	1.3809e-01	1.99	3.1342e-02	2.15	2.4469e+00	0.99
9282	3.4362e-02	2.01	7.8614e-03	2.00	1.2253e+00	1.00
37122	8.5043e-03	2.01	1.9695e-03	2.00	6.1290e-01	1.00

case $\partial\mathbf{S} \neq \emptyset$.

Example 3 *We now consider a surface* $\mathbf{S}$ *given by* $\mathbf{S} = \{\mathbf{x} \in \mathbb{R}^3 \mid (x_3 - x_2^2)^2 + x_1^2 + x_2^2 = 1, x_3 \geqslant x_2^2\}$ *(see [21]) with boundary*

$$\partial\mathbf{S} = \{(x_1, x_2, x_2^2 + \sqrt{1 - x_1^2 + x_2^2}) \mid x_1^2 + x_2^2 = 1\}.$$

The outward normal at $\mathbf{x} \in \mathbf{S}$ *is given by* $\vec{\mathbf{n}}(\mathbf{x}) = \vec{t}/\|\vec{t}\|$ *with* $\vec{t} = (x_1, x_2(1-2(x_3-x_2^2)), x_3 - x_2^2)$. *We let* $a(\mathbf{x}) = 1$, $b(\mathbf{x}) = 1$ *in (1.1), and let* $f = f(\mathbf{x})$ *be computed from (1.1) with an exact solution* u *given by* $u(\mathbf{x}) = x_1 x_2$. *We omit the long expression of* $v(\mathbf{x}) = -\Delta_s u$ *here. Dirichlet boundary conditions are used for both* u *and* v, *that is, both the values of* u *and* v *are specified on the boundary. We note that the norms of the exact solution are* $\|u\|_{L^2(\mathbf{S})} \approx 5.9370e-01$,

Table 4. Errors after gradient recovery on CCVDT meshes for Example 2.

Nodes	$\|\nabla_s u - Du^h\|_{L^2}$	CR	$\|\nabla_s u - Du^h\|_{H^1}$	CR	$\|\nabla_s(\nabla_s u) - D(Du^h)\|_{L^2}$	CR
147	1.2255e-01	-	5.3238e-01	-	8.0471e-01	-
582	2.0438e-02	2.60	1.7590e-01	1.61	1.9823e-01	2.04
2322	6.3133e-03	1.70	8.3223e-02	1.08	5.9256e-02	1.75
9282	1.9713e-03	1.68	4.0421e-02	1.04	1.7059e-02	1.80
37122	4.7626e-04	2.05	1.9961e-02	1.02	5.4669e-03	1.64
Nodes	$\|\nabla_s v - Dv^h\|_{L^2}$	CR	$\|\nabla_s v - Dv^h\|_{H^1}$	CR	$\|\nabla_s(\nabla_s v) - D(Dv^h)\|_{L^2}$	CR
147	1.2889e+01	-	1.0259e+02	-	1.2503e+02	-
582	3.2394e+00	2.01	3.2346e+01	1.68	4.7407e+01	1.41
2322	8.8754e-01	1.87	1.3171e+01	1.30	1.4832e+01	1.68
9282	2.2784e-01	1.96	6.0078e+00	1.13	3.9916e+00	1.89
37122	5.7434e-02	1.99	2.9194e+00	1.04	1.0381e+00	1.94

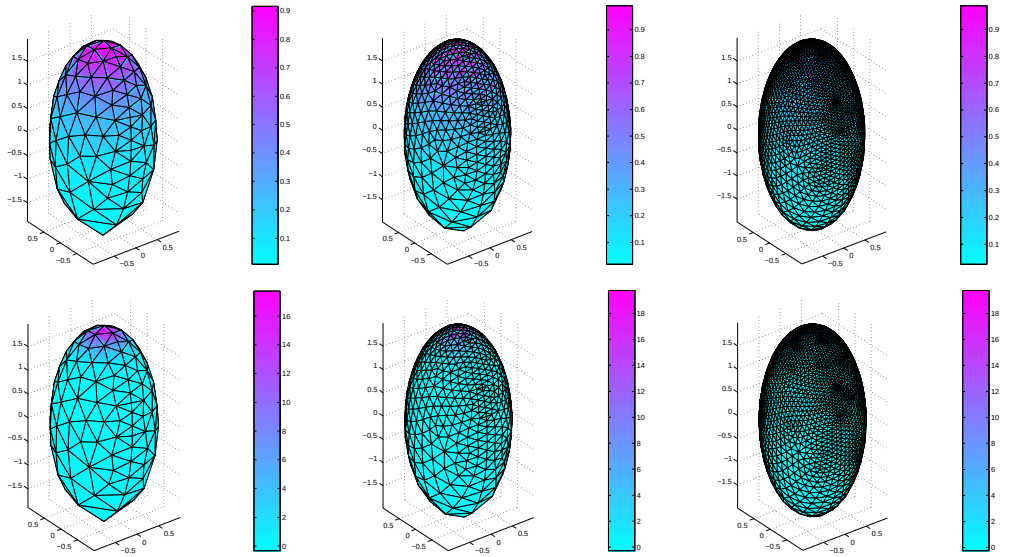

FIG. 3. Discrete solution u^h (top line) and v^h (bottom line) for Example 2 with $147, 582, 2322$ nodes respectively.

$\|u\|_{H^1(\mathbf{S})} \approx 1.6848e+00$, $\|u\|_{H^2(\mathbf{S})} \approx 5.6461e+00$, *and* $\|v\|_{L^2(\mathbf{S})} \approx 5.0840e+00$, $\|v\|_{H^1(\mathbf{S})} \approx 3.5017e+01$, $\|v\|_{H^2(\mathbf{S})} \approx 6.2741e+02$, *respectively.*

We solve the Example 3 numerically on six levels of CCVDT meshes with number of nodes n_i=64, 229, 865, 3361, 13429, and 52609, respectively. The uniform density function is used to generate the meshes. The corresponding h_{max} for each level mesh is 0.4597, 0.2719, 0.1482, 0.0834, 0.0469, and 0.0254, respectively. The computational results are reported in Tables 5 and 6. The meshes and corresponding discrete solutions are plotted in Figure 4. Although the analysis given in the paper is limited to problems defined on compact surfaces without boundary, the example shows similar results for some boundary value problems defined on a surface with

boundary. The analysis for the latter case is in fact very similar to the argument presented earlier for the compact surfaces. As for the gradient recovery scheme, the improvement in accuracy is not as dramatic as in the previous examples on the coarse meshes (the first few levels of CCDVT meshes), this is due to the fact that the coarse meshes lack sufficient resolution of the surface which experiences large curvature near the ends of the saddle so that it takes much larger number of nodes to obtain a well approximated surface. In addition, the gradient recovery scheme is intended for interior nodes only, thus the boundary contributions degrade the performance in the whole domain. As the resolution level increases, the surface starts to enjoy much better representation, and the percentage of boundary nodes gets smaller so that the boundary effect also becomes less significant, we thus witness a significant improvement in the accuracy for both recovered first and second order derivatives. These results demonstrate that the finite volume scheme can be used to accurately solve the high order PDEs on surfaces which in turn can be useful to the development of algorithms for evaluating various surface differential operators and geometric features.

Table 5. Computational results on CCVDT meshes for Example 3.

Nodes	$\|u-u^h\|_{L^\infty}$	CR	$\|u-u^h\|_{L^2}$	CR	$\|u-u^h\|_{H^1}$	CR
64	3.4891e-01	-	4.1019e-01	-	1.0509e+00	-
229	1.0850e-01	1.83	1.2908e-01	1.81	3.7107e-01	1.63
865	3.0600e-02	1.90	3.5866e-02	1.92	1.9550e-01	1.13
3361	1.0293e-02	1.61	1.2611e-02	1.54	5.6485e-02	1.59
13249	3.0648e-03	1.77	4.1839e-03	1.61	2.6754e-02	1.16
52609	1.2114e-03	1.35	1.1388e-03	1.89	1.3661e-02	0.97
Nodes	$\|v-v^h\|_{L^\infty}$	CR	$\|v-v^h\|_{L^2}$	CR	$\|v-v^h\|_{H^1}$	CR
64	4.9721e+00	-	2.8463e+00	-	2.8540e+01	-
229	3.8301e+00	0.41	1.2978e+00	1.23	2.3481e+01	0.31
865	1.1501e+00	1.81	2.7573e-01	2.33	1.1882e+01	1.03
3361	2.7514e-01	2.11	5.7805e-02	2.30	6.3983e+00	0.91
13249	8.9658e-02	1.63	1.4607e-02	2.01	3.2515e+00	0.99
52609	2.2372e-02	2.01	3.7421e-03	1.98	1.6320e+00	1.00

7. Conclusions

In this paper, we have studied a finite volume method for a model fourth order elliptic equations defined on a general smooth surface. Problems of the similar type often arise in various applications, and it is important to understand if the direct numerical discretization such as ones based on the finite volume methods can yield accurate approximation especially when high order differential operators on the surfaces are involved. Given a good approximation of the surface via planar triangulation and surface polygons, it is shown here that the H^1 error of the finite volume solution based on the splitting of the fourth order equation to second order systems is of optimal order, and thus provides accurate approximations to the solution of the PDEs. This gives a solid basis to the direct discretization approach for solving high order PDEs on surfaces. Moreover, when a constrained centroidal Voronoi tessellation based mesh is avail-

Table 6. Errors after gradient recovery on CCVDT meshes for Example 3.

Nodes	$\|\nabla_s u - Du^h\|_{L^2}$	CR	$\|\nabla_s u - Du^h\|_{H^1}$	CR	$\|\nabla_s(\nabla_s u) - D(Du^h)\|_{L^2}$	CR
64	7.9621e-01	-	4.4582e+00	-	4.4493e+00	-
229	2.1090e-01	2.08	2.7598e+00	0.75	3.1881e+00	0.52
865	6.3686e-02	1.80	1.4818e+00	0.94	1.7736e+00	0.88
3361	1.9217e-02	1.77	7.9686e-01	0.91	6.6433e-01	1.45
13249	5.4050e-03	1.85	4.5635e-01	0.81	2.9426e-01	1.18
52609	1.4961e-03	1.86	2.3355e-01	0.97	1.1630e-01	1.34
Nodes	$\|\nabla_s v - Dv^h\|_{L^2}$	CR	$\|\nabla_s v - Dv^h\|_{H^1}$	CR	$\|\nabla_s(\nabla_s v) - D(Dv^h)\|_{L^2}$	CR
64	3.4145e+01	-	9.6583e+02	-	3.6742e+02	-
229	2.2327e+01	0.67	6.0687e+02	0.73	6.2435e+02	-0.83
865	1.3986e+01	0.70	4.2536e+02	0.53	4.8619e+02	0.38
3361	5.7330e+00	1.31	2.2209e+02	0.95	3.1188e+02	0.65
13249	1.7685e+00	1.71	8.9703e+01	1.32	1.2932e+02	1.28
52609	4.7255e-01	1.91	3.7809e+01	1.25	3.9400e+01	1.72

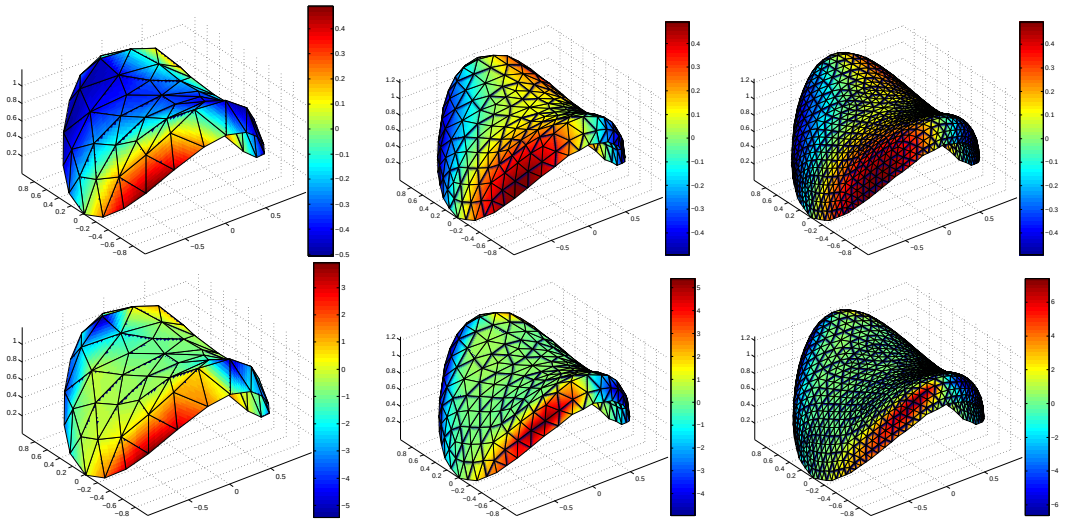

FIG. 4. Discrete solution u^h (top line) and v^h (bottom line) for Example 3 with $64, 229, 865$ nodes respectively.

able [17], they can provide highly accurate surface approximations. Based on such CCVDT meshes, a superconvergent gradient recovery can be efficiently and effectively constructed so that high order derivatives of the numerical solutions can enjoy high resolution (although only numerically demonstrated), which in turn may be useful when additional geometry manipulation and information processing are needed in practical applications. We conclude by taking note that the present study serves as an initial exploration of the application of finite volume methods to solve PDEs defined on general surfaces. The analysis is limited to a simple model equation, and it is given under the assumption that the surface can be discretized via a surface mesh consisting of piecewise planar triangles and its dual piecewise surface polygons. It will be

an interesting issue to examine if it is possible to simplify the construction of the dual meshes and to relax the requirement on their approximation properties in practice. Connections of the finite volume scheme with standard and other type finite element methods that are known for second order equations in the Euclidean space [3, 14] may also be considered for high order PDEs on surfaces. More challenging problems concerning the extensions to more complex nonlinear PDEs defined on deformable and possibly self-intersecting or singular surfaces also remain to be studied in the future, along with the study of problems where the definitions of the PDE and the underlying surface are coupled together so they may evolve simultaneously. More computational benchmark studies are also desirable, especially in settings where the surfaces may undergo topological changes and are thus perhaps more appealing to an implicit representation, to make comparisons of the direct finite volume discretization with other discretization methods.

Acknowledgement. The authors are very grateful to the referees for their careful reading of the manuscript and their valuable suggestions.

References

[1] T. Aubin (1982), *Nonlinear Analysis on Manifolds, Monge-Apmere Equations*, New York-Heidelberg-Berlin.

[2] C. Bajaj and G. Xu (2003), Anisotropic diffusion of subdivision surfaces and functions on surfaces, *ACM Trans. Graph.*, **22**, 4–32.

[3] R. Bank and D. Rose (1987), Some error estimates for the box method, *SIAM Journal of Numerical Analysis*, **24**, 777–787.

[4] J. Baranger, J. Maitre and F. Oudin (1996), Connection between finite volume and mixed finite element methods, *Model. Math. Anal. Numer*, **30**, 445–465.

[5] M. Bertalmio, L.-T. Cheng, S. Osher and G. Sapiro (2001), Variational methods and partial differential equations on implicit surfaces. *J. Comput. Phys.*, **174**, 759–780.

[6] A. Bertozzi, S. Esedoglu and A. Gillette (2007), Inpainting of binary images using the Cahn-Hilliard equation, *IEEE Trans. Image Proc.*, **16**, 285–291.

[7] M. Bloor and M. Wilson (2000), Method for efficient shape parameterization of fluid membranes and vesicles, *Phys. Rev. E*, **61**, 4218–4229.

[8] M. Burger (2006), Finite Element Approximation of Elliptic Partial Differential Equations on Implicit Surfaces, Computing and Visualization in Science.

[9] Z. Cai, J. Mandel and S. McCormick (1991), The finite volume element method for diffusion equations on general triangulations, *SIAM J Numer Anal.*, **28**, 392–403.

[10] S. Chou, D. Kwak and P. Vassilevski (1998), Mixed covolume methods for elliptic Problems on triangular grids, *SIAM Journal on Numerical Analysis*, **35**, 1850–1861.

[11] S. Chou and Q. Li (2000), Error estimates in L^2, H^1 and L^∞ in covolume methods for elliptic and parabolic problems: a unified approach, *Math. Comp.*, **69**, 103–120.

[12] U. Clarenz, U. Diewald and M. Rumpf (2000), Anisotropic geometric diffusion in surface processing, *Proceedings of IEEE Visualization*, 397–405.

[13] Y. Coudière, T. Gallouët, and R. Herbin (2001), Discrete Sobolev inequalities and L^p error estimates for finite volume solutions of convection diffusion equations, *Math. Model. Numer. Anal.* **35**, 767–778.

[14] J. Croisille (2000), Finite volume box schemes and mixed methods, *Math. Model. Numer. Anal.*, **34**, 1087–1106.

[15] J. Droniou and R. Eymard (2006), A mixed finite volume scheme for anisotropic diffusion problems on any grid, *Numerische Mathematik*, **105**, 35–71.

[16] Q. Du, V. Faber and M. Gunzburger (1999), Centroidal Voronoi tessellations: Applications and algorithms, *SIAM Review*, **41**, 37–676.

[17] Q. Du, M. Gunzburger and L. Ju (2003), Constrained centroidal Voronoi tessellations on general surfaces, *SIAM J. Sci. Comput.*, **24**, 1488–1506.

[18] Q. Du and L. Ju (2005), Finite volume methods on spheres and spherical centroidal Voronoi meshes, *SIAM J. Numer. Anal.*, **43**, 1673–1692.

[19] Q. Du, C. Liu and X. Wang (2004), A phase field approach in the numerical study of the elastic bending energy for vesicle membranes, *J. Comput. Phy.*, **198**, 450–468.

[20] Q. Du and D. Wang (2005), Anisotropic centroidal Voronoi tessellations and their applications, *SIAM J. Sci. Comp.*, **26**, 737–761.

[21] G. Dziuk (1988), Finite elements for the Beltrami operator on arbitrary surfaces, *Partial Differential Equations and Calculus of Variations*, ed. by S. Hildebrandt and R. Leis, *Lecture Notes in Mathematics*, **1357**, Springer, Berlin, 142–155.

[22] G. Dziuk and C. M. Elliot (2007), Finite elements on evolving surfaces, *IMA J. Numer. Anal.*, **27**, 262–292.

[23] G. Dziuk and C. M. Elliot (2007), Surface finite elements for parabolic equations, *J. Comput. Math.*, **25(4)**, 385–407.

[24] R. Ewing, R. Lazarov and Y. Lin (2000), Finite volume element approximations of nonlocal reactive flows in porous media, *Numerical Methods for PDEs*, **16**, 285–311.

[25] R. Eymard, T. Gallouet and R. Herbin (2006), A cell-centred finite-volume approximation for anisotropic diffusion operators on unstructured meshes in any space dimension, *IMA Journal of Numerical Analysis*, **26**, 326–353.

[26] F. Feng and W. Klug (2006), Finite element modeling of lipid bilayer membranes, *J. Comp. Phys.*, **220**, 394–408.

[27] T. Gallouët, R. Herbin and M. Vignal (2000), Error estimates on the approximate finite volume solution of convection diffusion equations with general boundary conditions, *SIAM J. Numer. Anal.* **37**, 1935–1972.

[28] J. Greer, A. Bertozzi and G. Sapiro (2006), Fourth order partial differential equations on general geometries, *J. Comput. Physics*, **216**, 216–246.

[29] E. Grinspun, Y. Gingold, J. Reisman and D. Zorin (2006), Computing discrete shape operators on general meshes, *Eurographics*, **25**.

[30] E. Hebey (2000), *Nonlinear Analysis on Manifolds: Sovolev Spaces and Inequalities*, AMS.

[31] G. Huiskamp (1991), Difference formulas for the surface Laplacian on a triangulated surface *J. Comp. Phys.*, **95**, 477–496.

[32] R. Lazarov, I. Mishev and P. Vassilevski (1996), Finite volume methods for convection-diffusion problems, *SIAM J. Numer. Anal.*, **33**, 31–55.

[33] R. Li, Z. Chen and W. Wu (2000), *Generalized Difference Methods for Differential Equations: Numerical Analysis of Finite Volume Methods*, Marcel Dekker, New York.

[34] M. Meyer, M. Desbrun, P. Schröder and A. Barr (2003), Discrete Differential-Geometry Operators for Triangulated 2-Manifolds, In *Visualization and Mathematics, III* , H. Hege and K. Polthier, Eds. Springer-Verlag, Heidelberg, 35–57.

[35] T. Myers, J. Charpin and S.J. Chapman (2002), The flow and solidification of a thin fluid film on an arbitrary three-dimensional surface, *Phys. Fluids*, **14**, 2788–2803.

[36] K. Morton and E. Süli (1991), Finite volume methods and their analysis. *IMA Journal of Numerical Analysis*, **11**, 241–260.

[37] R. Nicolaides (1992), Direct discretization of planar div-curl problems, *SIAM J. Numer. Anal.* **29**, 32–56.

[38] A. Ratz and A. Voigt (2006), PDE's on surfaces – a diffuse interface approach *Comm Math Sci*, **4**, 575–590.

[39] P. Smereka (2003), Semi-implicit level set methods for curvature and surface diffusion motion, *J. Sci. Comput*, **19**, 439–456.

[40] J. Stam (2003), Flows on surfaces of arbitrary topology, *ACM Transactions On Graphics*, **22**, 724–731.

[41] J. Thomas and D. Trujillo (1999), Mixed finite volume methods, *Inter. J. Numer. Methods Eng.*, **46**, 1351–1366.

[42] A. Toga (1998), Brain Warping, Academic Press, New York.

[43] T. Wang (2004), A mixed finite volume element method based on rectangular mesh for biharmonic equations, *J. Comput. Appl. Math.*, **172**, 117–130.

[44] H. Wu and R. Li (2003), Error estimates for finite volume element methods for general second-order elliptic problems, *Numerical Methods for PDEs*, **19**, 693–708.

[45] G. Xu, Q. Pan and C. Bajaj (2006), Discrete surface modelling using partial differential equations, *Computer Aided Geometric Design*, **23**, 125-145.

[46] J. Xu and H. Zhao (2003), An Eulerian formulation for solving partial differential equations along a moving interface, *J. Sci. Comput.*, **19**, 573–594.